MICROCOPY RESOLUTION TEST CHART
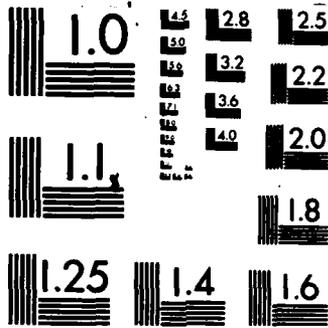NATIONAL BUREAU OF STANDARDS-1963-A

AD A137837

⑫

DOT/FAA/CT-82/149

Antimisting Fuel Breakup and Flammability

P. Parikh
R. Fleeter
V. Sarohia

December 1983

Final Report

DTIC
ELECTE
FEB 1 3 1984
S
E
D

US Department of Transportation

Federal Aviation Administration

Technical Center
Atlantic City Airport, N.J 08405

84 02 13 002

NOTICE

1. Report No. DOT/FAA/CT-82/149	2. Government Accession No. AD-A132832	3. Recipient's Catalog No.

4. Title and Subtitle	5. Report Date
Antimisting Fuel Breakup and Flammability	December 1983
	6. Performing Organization Code

7. Author(s) P. Parikh, R. Fleeter, and V. Sarohia	8. Performing Organization Report No.

9. Performing Organization Name and Address	10. Work Unit No.
JET PROPULSION LABORATORY California Institute of Technology 4800 Oak Grove Drive Pasadena, California 91109	11. Contract or Grant No. DTFA03-80-A-00215
	13. Type of Report and Period Covered Final August 1981-1982

12. Sponsoring Agency Name and Address U.S. Department of Transportation Federal Aviation Administration Technical Center Atlantic City, NJ 08405	14. Sponsoring Agency Code

15. Supplementary Notes

16. Abstract

The breakup behavior and flammability of antimisting turbine fuels subjected to aerodynamic shear are investigated in this report. Fuels tested were Jet A containing 0.3% FM-9 polymer (developed by ICI Americas) at various levels of degradation ranging from virgin AMK to neat Jet A. The misting behavior of the fuels was quantified by droplet size distribution measurements. A new technique based on high resolution laser photography and digital image processing of photographic records for rapid determination of droplet size distribution was developed for this purpose. The flammability of flowing droplet-air mixtures was quantified by direct measurements of temperature rise in a flame established in the wake of a continuous ignition source. The temperature rise measurements were correlated with droplet size measurements. The flame anchoring phenomenon associated with the breakup of a liquid fuel in the wake of a bluff body was shown to be important in the context of a survivable crash scenario. A new pass/fail criterion for flammability testing of antimisting fuels, based on this flame-anchoring phenomenon, was proposed. The role of various ignition sources and their intensity in ignition and post-ignition behavior of antimisting fuels was also investigated. Finally, the rate of flame spread on the surface of a pool of Jet A and AMK fuels was investigated for various depths of fuel layer at ambient temperature conditions.

17. Key Words (Selected by Author(s))	18. Distribution Statement
Aircraft Fires Antimisting Fuels Broadbase Fuels Combustion and Flammability	This document is available to the U.S. public through the National Technical Information Service, Springfield, Virginia 22161

19. Security Classif. (of this report) Unclassified	20. Security Classif. (of this page) Unclassified	21. No. of Pages	22. Price

JPL 0184 11/80

HOW TO FILL OUT THE TECHNICAL REPORT STANDARD TITLE PAGE

Make items 1, 4, 5, 9, 12, and 13 agree with the corresponding information on the report cover. Use all capital letters for title (item 4). Leave items 2, 6, and 14 blank. Complete the remaining items as follows:

3. Recipient's Catalog No. Reserved for use by report recipients.

7. Author(s). Include corresponding information from the report cover. In addition, list the affiliation of an author if it differs from that of the performing organization.

8. Performing Organization Report No. Insert if performing organization wishes to assign this number.

10. Work Unit No. Use the agency-wide code (for example, 923-50-10-06-72), which uniquely identifies the work unit under which the work was authorized. Non-NASA performing organizations will leave this blank.

11. Insert the number of the contract or grant under which the report was prepared.

15. Supplementary Notes. Enter information not included elsewhere but useful, such as: Prepared in cooperation with... Translation of (or by)... Presented at conference of... To be published in...

16. Abstract. Include a brief (not to exceed 200 words) factual summary of the most significant information contained in the report. If possible, the abstract of a classified report should be unclassified. If the report contains a significant bibliography or literature survey, mention it here.

17. Key Words. Insert terms or short phrases selected by the author that identify the principal subjects covered in the report, and that are sufficiently specific and precise to be used for cataloging.

18. Distribution Statement. Enter one of the authorized statements used to denote releasability to the public or a limitation on dissemination for reasons other than security of defense information. Authorized statements are "Unclassified—Unlimited, " "U. S. Government and Contractors only, " "U. S. Government Agencies only, " and "NASA and NASA Contractors only. "

19. Security Classification (of report). NOTE: Reports carrying a security classification will require additional markings giving security and downgrading information as specified by the Security Requirements Checklist and the DoD Industrial Security Manual (DoD 5220.22-M).

20. Security Classification (of this page). NOTE: Because this page may be used in preparing announcements, bibliographies, and data banks, it should be unclassified if possible. If a classification is required, indicate separately the classification of the title and the abstract by following these items with either "(U)" for unclassified, or "(C)" or "(S)" as applicable for classified items.

21. No. of Pages. Insert the number of pages.

22. Price. Insert the price set by the Clearinghouse for Federal Scientific and Technical Information or the Government Printing Office, if known.

ACKNOWLEDGEMENTS

Accession For

NTIS GRA&I	X
DTIC TAB	☐
Unannounced	☐
Justification	

By

Distribution/

Availability Codes

| Dist | Avail and/or Special |

A-1

TABLE OF CONTENTS

PREVIOUS PAGE
IS BLANK

LIST OF FIGURES

LIST OF TABLES

EXECUTIVE SUMMARY

The breakup behavior and flammability of antimisting turbine fuels subjected to aerodynamic shear are investigated in this report. Fuels tested were Jet A containing 0.3 percent FM-9 polymer (developed by ICI Americas) at various levels of degradation ranging from virgin AMK to neat Jet A. The shearing air speeds employed ranged from 20 to 80 m/s (40 to 160 knots).

The misting behavior of the fuels was quantified by droplet size distribution measurements. A new technique based on high resolution laser photography and digital image processing of photographic records for rapid determination of droplet size distribution was developed for this purpose. The flammability of flowing droplet-air mixtures was quantified by direct measurements of temperature rise in a flame established in the wake of a continuous ignition source. The temperature rise measurements were correlated with droplet size measurements. The mist flammability, defined in terms of a reduced temperature, was found to be a function primarily of the mist SMD and was independent of the fuel dump rate.

The flame anchoring phenomenon associated with the breakup of a liquid fuel in the wake of a bluff body following ignition by a transient source was shown to be important in the context of a survivable crash scenario. A new pass/fail criterion for flammability testing of antimisting fuels, based on this flame-anchoring phenomenon, was proposed. Pass/fail boundary based on this criterion was found to be a strong function of both the airspeed and the degree of fuel degradation as measured by the filter ratio. Within the range of the fuel dump rates employed (10 to 40 gpm), it was not possible to have a self-supporting flame anchored in the wake of a bluff body (fail condition) for fuels having filter ratio larger than 8 and air speeds lower than 160 knots.

The role of various ignition sources and their intensity in ignition and post-ignition behavior of antimisting fuels was also investigated. It was found that the ignition source intensity plays a key role in determining whether or not ignition of a given droplet-air mixture will be achieved. The threshold ignition intensities to achieve ignition of various filter ratio fuels aerodynamically misted by a 100 knot wind were determined. Over a wide range of fuel dump rates and ignition source intensities in the present laboratory scale experiments, the proposed pass/fail criterion based on the flame anchoring phenomenon was found to be independent of the fuel dump rate and the ignition source intensity.

Finally, the rate of flame spread on the surface of a pool of Jet A and AMK fuels was investigated for various depths of fuel layer at ambient temperature condition. Within the uncertainty of the data, no significant difference between the flame spread rate over pools of Jet A and AMK fuels was observed. The flame spread rate generally increased from about 2 cm/sec to 3.5 cm/sec as the depth of the fuel layer was increased from 3 mm to 18 mm. The presence of a porous substrate (such as loosely packed soil) inhibits flame spread. Steady state flame spread over a fuel soaked bed of sand was 1/5 to 1/6 of the measured spread rate for a pure liquid layer.

ix

1. INTRODUCTION

Fire related fatalities resulting from postcrash fires in otherwise survivable aircraft crashes are of a major concern to turbine powered commercial aircraft operations. Approximately 40 percent of the fatalities in such crashes are attributable to fire and fire-related effects (reference 1). Most postcrash fires are fuel-fed and the mechanism of their initiation, propagation and growth has been a subject of many investigations. Although a multiplicity of scenarios is possible, the most probable cause of a postcrash fuel fire has been identified as moderate to massive fuel spillage due to wing separation or fuel tank rupture during the dynamic phase of an impact survivable crash (references 1, 2). Currently employed commercial aircraft turbine fuels such as Jet A have typical wing tank temperatures well below the flash point and are difficult to ignite in bulk quantities. However, under dynamic crash conditions, when such fuels are released in moderate to large quantities from ruptured fuel tanks into a high speed airstream, they break up into fine droplets, thereby forming a highly flammable mist. This fuel mist is readily ignited by one or more of the numerous transient ignition sources such as friction sparks, electrical sparks, hot engine parts, etc. A rapid propagation of fire from transient ignition source to the point of fuel release occurs, accompanied by the development of a large fireball throughout the region of fuel mist. The fireball serves as a large ignition source that ignites pools of liquid fuel around the aircraft as it decelerates to a stop. The resulting pool fire is fed by additional fuel leaking from the damaged tanks and in some instances the rapid heating of undamaged fuel tanks results in explosions (references 1, 2).

A necessary precursor to the above chain of events in the development of a postcrash fire scenario is the misting tendency of the currently employed turbine fuels as they are released in a high speed airstream. If this misting can be suppressed sufficiently, the probability of ignition by transient ignition sources and subsequent fireball formation may be greatly reduced or eliminated, thereby preventing the entire large-scale, postcrash fire scenario. Polymer additives that impart such an antimisting property to currently employed turbine fuels have been developed over the last several years. An antimisting fuel offers its potential safety advantages during the short but critical dynamic (deceleration) phase of a survivable crash, thereby negating the entire postcrash, large-scale fire scenario.

With the development of polymer fuel additives that suppress the misting tendency, a need has arisen for the development of proper flammability test methods and meaningful pass/fail criteria to evaluate the fire suppression performance of these new antimisting fuels. Existing flammability criteria such as the flash point temperature are inadequate for this purpose. The use of flashpoint temperature to rate the flammability of various antimisting fuels containing the same base fuel (Jet A) but different additives (FM-9, AM-1, etc.) would lead to the erroneous conclusion that all antimisting fuels in this category are equally flammable, since the flash point temperature is not altered by the additives. The point is that any flammability test to evaluate the fire suppression performance of antimisting fuels should be realistic and should simulate as closely as possible the conditions that prevail during an actual crash.

Some insight into the events that lead to a large scale, postcrash fire scenario in a survivable crash may be gained from the NTSB accident reports

1

(references 3, 4) on such crashes. However, a more detailed understanding of the mechanisms involved may be gained from simulated full-scale crash tests conducted by the FAA (reference 5). The sequence of events is well-documented in motion pictures and important dynamic parameters may be measured. A review of the Lakehurst crash No. 1 (reference 5) conducted with Jet A fuel reveals that the following two aspects of the dynamic phase of a survivable crash scenario are important:

1) Fuel has a tendency to form a mist when released in a high speed airstream.

2) The mist, ignited by a transient ignition source (a smudge pot flame on the ground in this case) supports a stable flame which travels with the aircraft and engulfs the aircraft as it decelerates to a stop.

The second aspect is important because a stable flame anch   d near the point of fuel release and traveling with the aircraft provides   ۱arge ignition source that ignites pools of fuel on the ground and le   to a large-scale, postcrash fire. It also provides a guideline for   ۷   ٰng a flammability test on how much we need to suppress the misting. '   ٰously, we need to suppress the misting tendency of the fuel to a point where anchoring of a self-supporting flame near the fuel release location is not possible, following ignition by a transient ignition source.

Ignition sources that occur during the dynamic phase of a survivable crash include transient sources such as electrical or friction sparks or continuous ones such as torching engine ingesting fuel (Reference 1, page 5-6). In the presence of a large ignition source such as a torching engine, the possibility of igniting the released fuel, whether Jet A or AMK, may not be avoided. However, the resulting fire is far more likely to remain localized with AMK, in contrast with Jet A which is likely to result in a fireball.

Flame spread on the free surface of a pool of liquid fuel following local ignition is of considerable interest and relevance to the postcrash fire scenario. In many instances, this flame spread rate determines the growth rate of the fire intensity and consequently the length of time available for safe evacuation of survivors from the crash scene. For high flash point fuels such as Jet A, the environmental and bulk fuel temperatures are usually lower than the flash point temperature. Consequently, the flame spreading rate on a liquid surface is much smaller than that for low flashpoint fuels such as gasoline. For the latter type of fuels a combustible mixture of fuel vapors and air already exists near the liquid surface, even at normal environmental temperatures (i.e., their flash point temperature is lower than the environmental temperature). As shown by Mackinven et al. (reference 6), for high flash point fuels such as Jet A, convection within the liquid layer is the principal mechanism by which fuel ahead of the flame front is heated up to the flash point temperature. As the addition of polymers to suppress the misting behavior of aviation turbine fuels essentially alters the rheology of such fuels, such additives may be expected to influence the flame spreading behavior on the surface of a fuel pool.

The JPL program on the investigation of the flammability of AMK fuel was designed to address all these important aspects of a survivable crash scenario. First, the misting behavior of fuels released in a high speed airstream was quantified by means of droplet size distribution and population measurements. A new technique based on high resolution laser photography and digital image processing of photographic records for rapid determination of droplet size distribution was developed for this purpose. Second, the flammability of a flowing droplet-air mixture was quantified by direct measurements of temperature rise in a flame established in the wake of a continuous ignition source. The temperature rise measurements were correlated with the droplet size measurements to demonstrate the role of misting in the flammability of droplet-air mixtures. Third, the flame anchoring phenomenon associated with the breakup of a liquid fuel in the wake of a bluff body was investigated and a new pass/fail criterion for flammability testing of antimisting fuels was proposed. The role of various ignition sources and their intensity in ignition and post-ignition behavior of antimisting fuels was also investigated.

Finally, the flame spreading rate on the surface of pools of Jet A and AMK fuels was investigated for various depths of the fuel layer at the ambient temperature condition.

The experimental configuration and results for each of the above four investigations are described separately in the following three chapters of this report.

3

2. ATOMIZATION AND FLAMMABILITY MEASUREMENTS IN THE MINIWING SHEAR FACILITY

2.1 Problem Statement and Research Goals

Upon initiation of the AMK program at JPL it became clear that a quantitative measure of mist flammability was essential to meaningful comparison of experimental data. Both the relative flammability of a single fuel at various airspeeds and fuel ejection rates and the relative flammability of differing fuels under identical experimental conditions needed to be measured under realistic simulation of an impact-survivable aircraft crash. Finally, results of large-scale FAA Wing Shear tests were to be compared with a smaller-scale test to investigate size scaling effects. For these reasons the miniwing shear experiment described in detail by Fleeter et al. (reference 7) and shown schematically in figure 2-1 was designed, built, and operated. Quantification of the relative flammability of the fuel mists produced was accomplished primarily with temperature measurements within the flame downstream of the continuous ignition source as shown in figure 2-1.

To isolate the antimisting quality of the fuel as the basis for differences observed in mist flammability, a system for analysis of the fuel sprays produced in the tests was devised, assembled and operated. This system, which incorporates digital analysis of high resolution, large field images produced under pulsed laser sheet illumination, has been described fully by Fleeter et al. (references 8, and 9). The major goal of this effort was to determine whether the measured flammability of various mists could be correlated with mist characteristics such as the mean diameter of the drops of which it is comprised. Through establishment of such a relation, future evaluation of both alternative fuels and new crash simulations could be affected solely by spray analysis without recourse to large scale crash tests.

It is noteworthy that both the spray mean diameter and the temperature data are obtained in the experiments as functions of airspeed, fuel dump rate and polymer concentration. They are not directly reduced to a pass/fail (yes/no) form. However, a greater amount of information is available from which numerical correlations may be made (e.g., between spray mean diameter and flammability). The reader is directed to appendix A for a further discussion of the basis for quantitative measurement of flammability and a definition of the reduced temperature Ɵ used in the following discussion.

2.2 Experimental Procedure

Fuel flammability as evaluated by reduced temperature, Ɵ was measured over a range of simulated crash airspeeds, fuel flow rates and antimisting polymer concentration. The latter was performed in response to questions during the experimental phase of the program concerning the feasibility of using decreased polymer concentration. The nominal conditions tested were airspeeds of 58, 81 and 98 m/s, fuel flow rates of 250, 500 and 750 grams/sec, and FM-9 concentrations of 0 (Jet A), 0.30, 0.25 and 0.20 percent. This results in an experimental matrix of 36 points. At each point, a flammability test with continuous ignition by an oxy-acetylene torch using the apparatus diagrammed in figure 2-1 was carried out. At a later time, the experimental conditions of air and fuel mass flow rate and temperature were
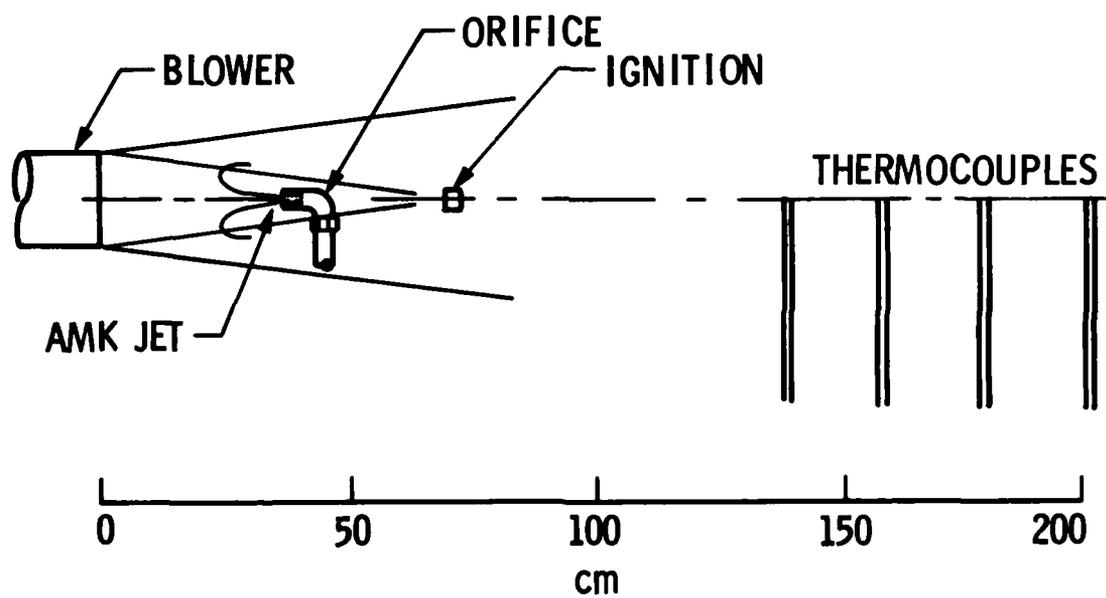
4

Figure 2-1.   Mini Wing Shear Apparatus for Flammability
Measurement

repeated with the same fuel composition. In this second series of tests, the system geometry was unchanged but no ignition was attempted. Instead the laser and camera were installed for photography of the fuel mist immediately downstream of the torch flange where ignition would have been attempted in the hot tests. In this way mist characterization results could be compared with flammability test results to seek any possible relationship of the two.

Spray characterization was mainly concerned with measurement of the mist Sauter Mean Diameter (SMD). The SMD is defined as

$$SMD = \frac{\sum D^3}{\sum D^2}$$

where D is the effective diameter of each drop and the sigmas imply summation over all the drops counted. The effective diameter, D, was defined in response to the ability of the image analysis system to measure drop cross sectional area most accurately. D was computed as the diameter of a hypothetical spherical drop possessing the same cross sectional area as the observed drop. In this way the physical meaning of the SMD, description of a spray in terms of the diameter of a spherical drop possessing the same volume-to-surface area ratio as that of the gross spray, was felt best preserved.

2.3 Results and Discussion

Tables 2-1 through 2-3 contain the tabulated data from 27 of the 36 test points. Jet A data (9 of the experimental points) are not tabulated because no SMD measurements were possible with this fuel under any of the conditions tested in the wing shear facility. Images formed showed almost no drops of diameter greater than 20 μm. Instead, the viewing field was filled with a fine, featureless mist which is assumed to be the image of a large number of drops smaller than the system resolution of 8 μm. One of these images is reproduced in figure 2-2 while a relatively finely atomized AMK mist is shown in figure 2-3 for comparison. Drops are clearly visible in the AMK spray Furthermore, flammability results for Jet A showed no appreciable variation in reduced temperature, θ with either airspeed or fuel ejection rate. Reduced temperature for these tests hovered consistently close to 0.60.

Drops of diameter greater than 500 μm play a large role in determination of AMK mist flammability. They contain a large fraction of the total fuel volume. For example, a single drop of 1000 μm diameter contains as much fuel as 8000 drops of 50 μm diameter. One such large drop has the same surface area as only 400 drops of 50 μm. Thus the free fuel surface available for fuel evaporation is 20 times greater for fuel contained in 50 μm drops than for the same volume of fuel contained in a 1000 μm drop. It is for this reason that a system was devised capable of observing the widest possible range of drop size. The SMD values shown in the tables were computed from measurement of drops of diameter from 8 to 2000 μm. The relative population of large drops is rather small. Typically in a spray section containing 450

6

drops, 350 of the drops are under 50 μm in diameter, even for 0.30 percent FM-9 AMK. The same spray is likely to contain only two or three drops over 1000 μm diameter, and less than 20 drops over 500 μm diameter.

In considering where the bulk of the fuel is, these few large drops are very significant. A hypothetical spray of 400 drops of 20 μm diameter and 10 drops of 1000 μm diameter has 99.97 percent of the fuel in the ten large drops. The SMD for this spray would be 985 μm, reflecting the dominance of the 10 large drops out of the 410 drops counted. Despite their importance however, their relative scarcity means that not enough of them are counted to yield smooth population statistics. That is to say it is a matter of chance whether e.g., three rather than four large drops are observed in a sample of a negative. Observation of even 1 additional large drop may change the calculated SMD by several hundred microns (e.g., without the ten large drops the SMD of the hypothetical spray discussed above is reduced from 985 to 20 μm). This effect can only be eliminated by obtaining a large enough sample to observe a sufficient number of large drops to yield smooth statistics. This is not a practical solution as it requires counting about one hundred times as many drops as is done currently, a process requiring a man-week of work on each negative using the current system. Even such large-scale analytical effort might not yield smooth results as the breakup itself is inherently an unsteady process. An alternative is to artificially limit the maximum drop size to 1000 μm diameter from 2000 μm. This still permits sensitivity to most of the large drops carrying a significant portion of the fuel while eliminating those drops which by their random appearance distort statistical results.

Table 2-1. Mini Wing Shear Test Results: Jet A + 0.30 Percent FM-9

Airspeed m/s	Fuel Flowrate g/s	SMD (2000 μm maximum diameter) μm	SMD (1000 μm maximum diameter) μm	θ
55	175	1243 ±200	585 ±50	0.005
55	520	822 ±200	520 ±50	0.0026
55	660	1036 ±200	624 ±50	0.001
81	175	1060 ±300	564 ±75	0.020
81	520	666 ±300	494 ±75	0.023
81	660	1245 ±300	611 ±75	0.020
99	175	1000 ±400	656 ±130	0.030
99	520	571 ±400	571 ±130	0.024
99	660	1348 ±400	401 ±130	0.018

7

Table 2-2. Mini Wing Shear Test Results: Jet A + 0.25 Percent FM-9

Airspeed m/s	Fuel Flowrate g/s	SMD (2000 μm maximum diameter) μm	SMD (1000 μm maximum diameter) μm	θ
58	230	701 ±200	576 ±35	0.006
58	400	1045 ±200	510 ±35	0.005
58	750	659 ±200	525 ±35	0.003
81	230	940 ±150	439 ±35	0.015
81	400	841 ±150	482 ±35	0.015
81	750	644 ±150	417 ±35	0.017
98	230	808 ±200	425 ±100	0.030
98	400	471 ±200	327 ±100	0.038
98	750	794 ±200	498 ±100	0.035

Table 2-3. Mini Wing Shear Test Results: Jet A + 0.20 Percent FM-9

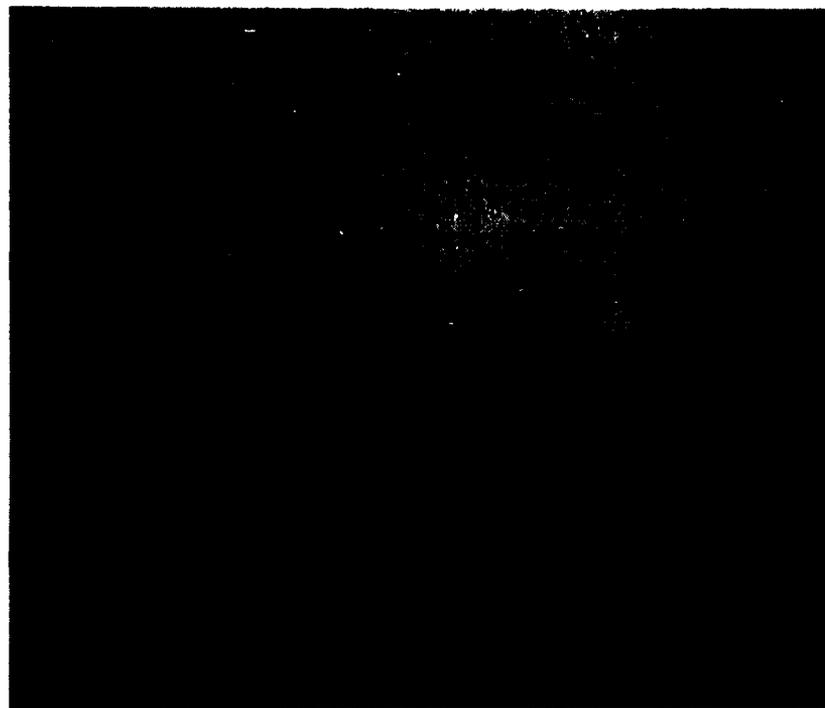| Airspeed m/s	Fuel Flowrate g/s	SMD (2000 μm maximum diameter) μm	SMD (1000 μm maximum diameter) μm	θ
58	330	970 ±170	525 ±60	0.01
58	610	1132 ±170	632 ±60	0.006
58	840	788 ±170	541 ±60	0.007
82	330	691 ±20	552 ±90	0.10
82	610	723 ±20	556 ±90	0.36
82	840	700 ±20	402 ±90	0.10
99	330	864 ±260	354 ±40	0.10
99	610	384 ±260	385 ±40	0.10
99	840	439 ±260	429 ±40	0.10

8

Figure 2-2. Mist Formed by Atomization of Jet A at 97 m s^{-1}

Figure 2-3. Mist Formed by Atomization of Jet A + 0.20% FM-9 at 99 m s^{-1}

Calculation of spray SMD has been carried out over this reduced diameter range and the results appear in tables 2-1 through 2-3. The results of calculation with the 1000 μm limit compared with the normal 2000 μm limit are firstly a significant drop in the raw SMD values. In making flammability comparisons, SMD values calculated with different limits should not be compared with each other. The trends are similar but, as expected, much less scatter is evident in the data calculated with the lower limit.

None of the data shows any trend in SMD with changes in fuel dump rate. Thus, it was concluded that dump rate does not affect atomization directly. The data at each airspeed for each fuel tested taken at three dump rates may then be considered as a rough measure of experimental reproducibility. Standard deviations have been calculated from these measurements and are given both in the tables and subsequent figures as the error bands associated with the measurements. The average of the standard deviations was 211 μm for the full data set. This was reduced to 67 μm for the data set restricted to diameters under 1000 μm.

To examine the relationship of jet breakup and atomization to shearing air velocity, measured SMD values were averaged over the three fuel dump rates tested. This averaging allows the singling out of the effect of the experimental parameter of interest, in this case velocity, in data of inherently large scatter. The results depicted in figure 2-4 show a clear trend of decreasing SMD with increasing air velocity. The trends are significant for both the 1000 μm and 2000 μm maximum diameter data, though only the 1000 μm data are shown for clarity. While two of the 0.20 percent FM-9 data points are at slightly higher SMD values than the corresponding 0.25 percent FM-9 data, they lie within their mutual bands of uncertainty so no significance can be associated with the observation. If it were to prove significant, this trend could be explained by the tendency of the polymer to swell more (under zero shear) at lower concentrations. Thus under low shear (low airspeed) conditions it might appear to have greater antimisting ability. The lower concentration polymer is more fragile in its more expanded state, so the network of polymer chains is more easily ruptured, leading to a rapid diminishing of antimisting ability at higher shear (higher airspeed).

Figure 2-5 depicts the relationship of spray flammability to the fuel atomization as represented by the mist SMD computed using a maximum diameter of 2000 μm. A dependence is clearly present, supporting the assertion that the atomization behavior dominates mist flammability. These data span nearly a factor of two in shearing air velocity and more than a factor of four in fuel ejection rate. The correlation with SMD alone indicates that mist flammability has no strong dependence on the other experimental parameters except through their influence on the fuel atomization. For example, we see that the airspeed affects the flammability only because at higher airspeeds the fuel is more finely atomized.

The role of the drop mean diameter in mist flammability has been treated analytically and the details of this analysis are presented in appendix B. The result of this analysis is that for spray density which is low enough that drops burn individually (i.e. with an individual flame surrounding each drop

10
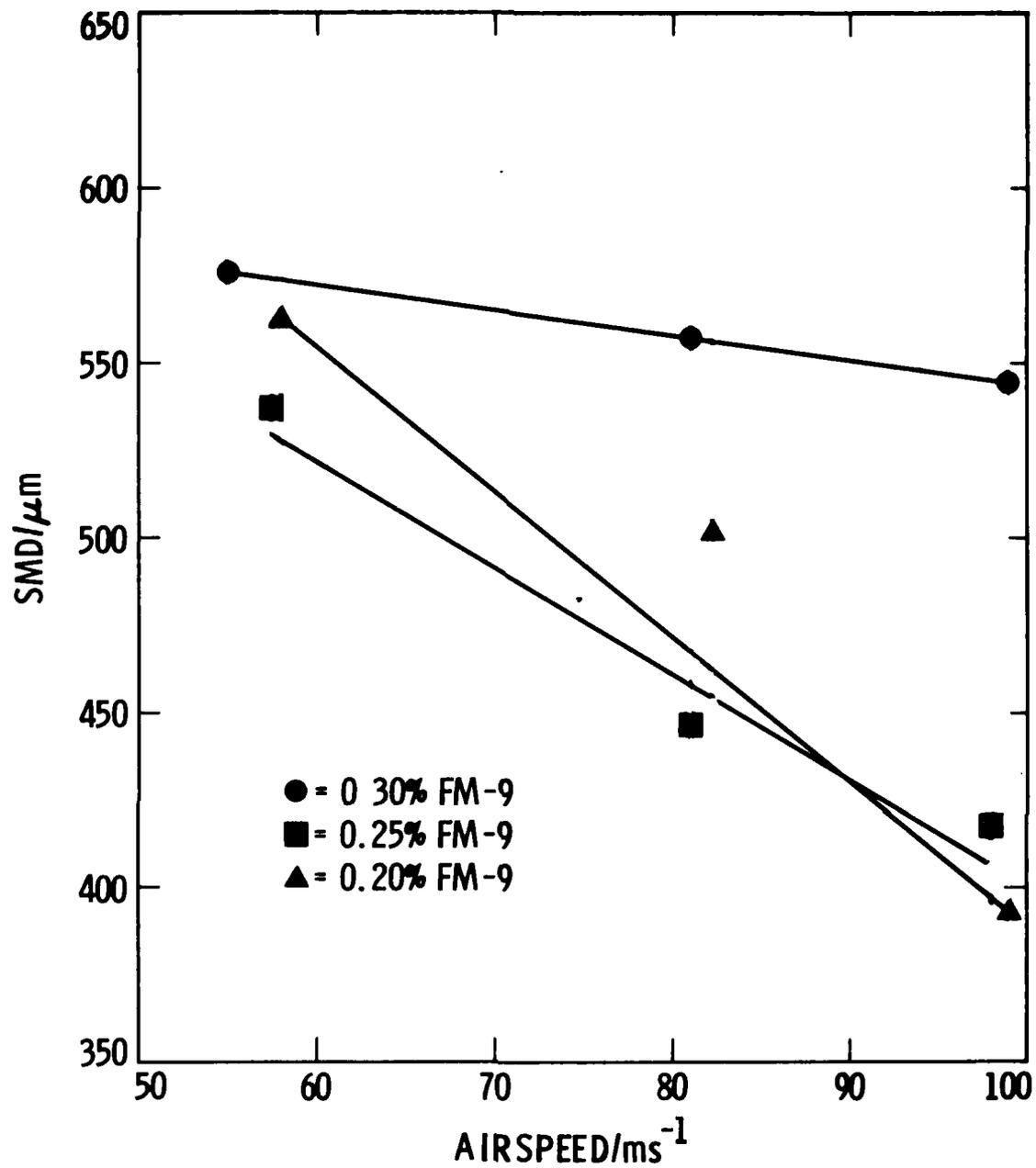
Figure 2-4. Fuel Atomization as a Function of Shearing
Airspeed. SMD values computed with a maximum
diameter of 1000 μm

11

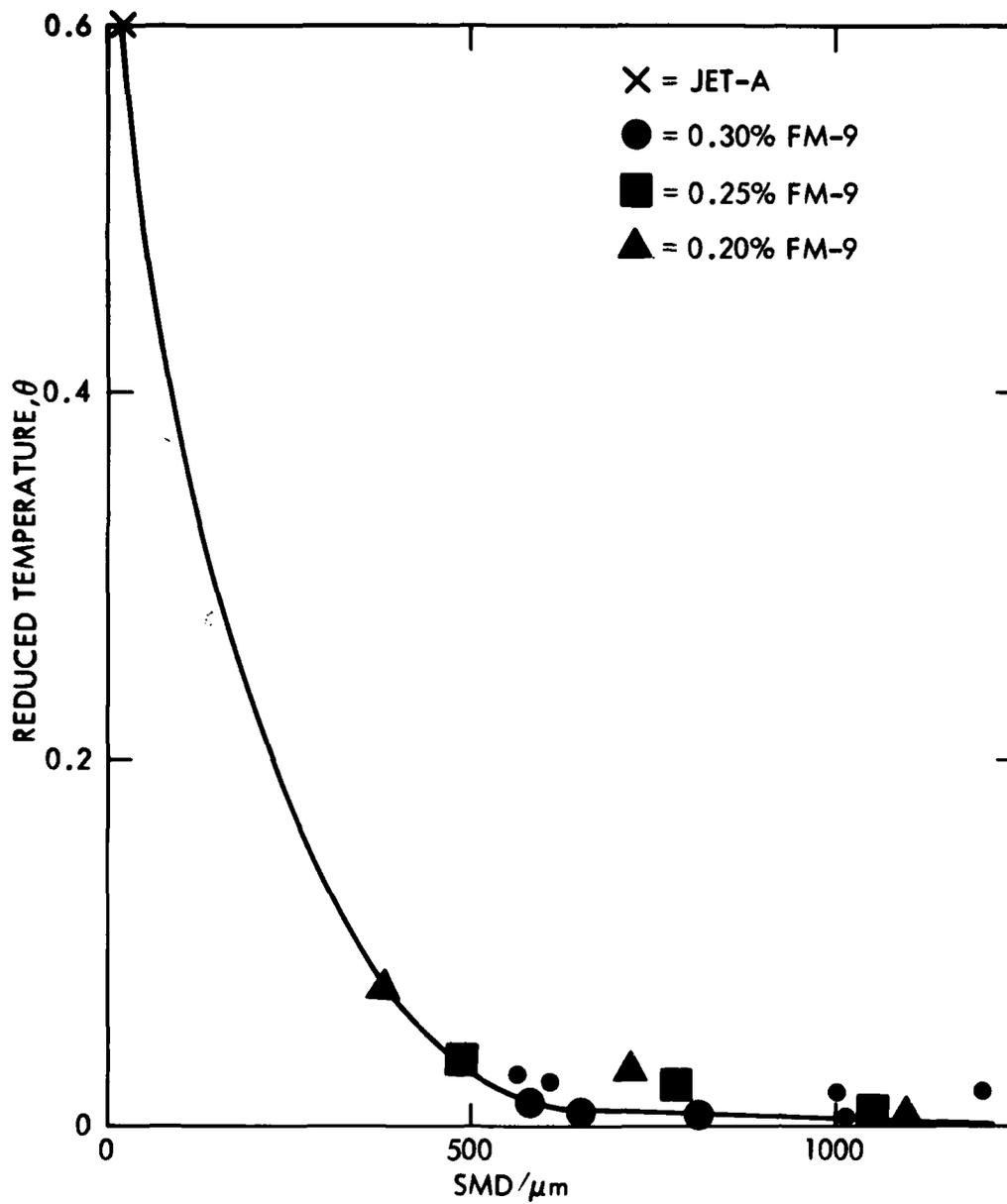Figure 2-5. Flammability as a Function of Fuel Atomization.
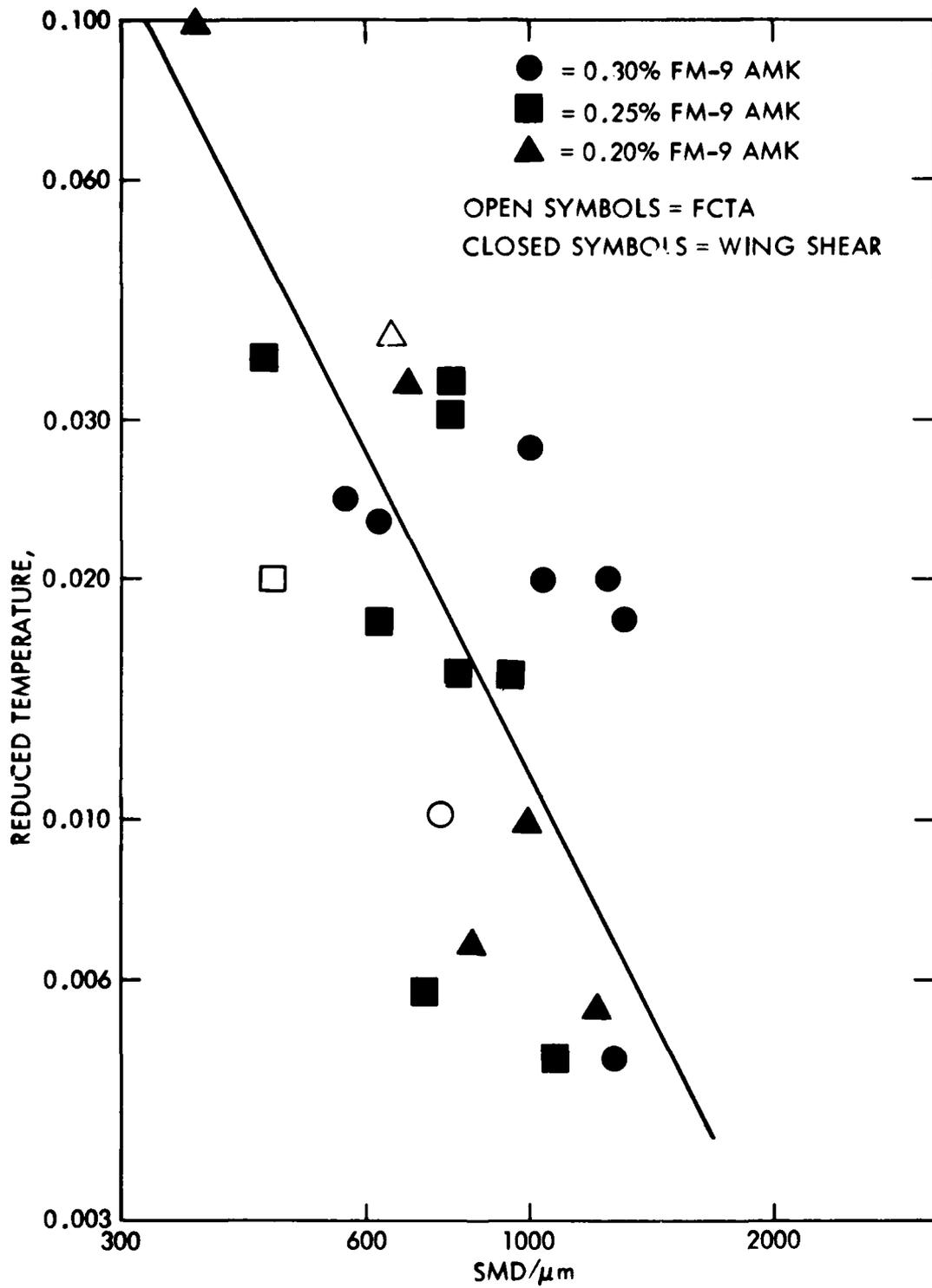SMD values computed with a maximum diameter of 2000 μm

12

Figure 2-6. Comparison of Theory (straight line) and Experimental Flammability Results Linking Spray Flammability to Mist SMD. (The repeatability of the temperature measurements used in calculation of θ is ±20%. SMD Measurements carry an estimated uncertainty of ±100 μm-see text.)

13

as opposed to a large flame sheet surrounding a cluster of drops), a simple relationship exists between flammability and mean drop size. This relationship is

$$\log \theta \ \alpha \ -2\log\overline{D}$$

where $\overline{D}$ is the spray SMD. Figure 2-6 shows the experimental data in a log/log format with the theoretically derived straight line relation. Experimental data are burdened with an uncertainty resulting from the assumptions inherent in the definition of the reduced temperature (see appendix A) and in measurement of spray SMD. The reproducibility of the temperature measurement used in calculation of θ was observed to be ±20 percent. The uncertainty in measurement of SMD is of the order of ±100 μm. This estimate is based on results from three repetitions of experiments using identical fuels and air flow rates but with varying fuel ejection rates. The experimental data exhibit a trend similar to that predicted by theory.

2.4 Conclusions

1) Mist flammability, as measured by reduced temperature, is a function of spray SMD. Parameters such as fuel ejection rate and shearing air velocity affect the flammability through their effect on atomization.

2) The flammability data exhibit trends similar to that predicted by the relation

$$\log \theta \ \alpha \ -2\log\overline{D}$$

where $\overline{D}$ is the spray SMD.

3. FLAME STABILIZATION AND FLAMMABILITY CRITERIA

3.1. Background and Literature Review

As mentioned in section 1 the existing test methods and criteria for evaluating the flammability of conventional turbine fuels are not suitable for testing antimisting fuels. New test methods and criteria within the context of a survivable crash scenario must be devised for such fuels. Several new test methods, all of which incorporate fuel droplet breakup by aerodynamic shear, have been developed over the years. Thus, all the new test methods incorporate the first important aspect of a survivable crash scenario discussed in section 1. However, the pass/fail criteria used in many of these tests are quite arbitrary. The tests thus serve as sorting tests, comparing the performance of one fuel with another on a certain scale peculiar to a given test. They do not provide a measure of the absolute fire resistance of the fuel as it relates to a survivable crash. One phase of AMK flammability work at JPL has been aimed at the development of an absolute pass/fail criterion, utilizing as a guideline the second important aspect of a survivable crash namely, the phenomenon of flame anchoring following ignition by a transient source as discussed in section 1. Before discussing the JPL work on the development of this pass/fail criterion of flammability, test methods and criteria employed by other investigators will first be reviewed.

Perhaps the most realistic flammability test is the RAE rocket sled test (reference 12). In this test, a wing shaped fuel tank is mounted on a sled and is accelerated to a desired speed along a track by means of rocket thrusters. The sled is then decelerated either by means of an arrester wire or by frictional means. In the "standard" test, decelerations as high as 10 to 25 g's are applied by means of the arrester wire, while "run on" tests employ frictional braking and produce decelerations of the order of 1 g. Fuel is allowed to spew out from a hole or slit in the leading edge of the wing tank during deceleration. In the "standard" test, the fuel is flung forward onto an array of ignition sources ahead of the sled, while in "run on" tests the sled passes in the vicinity of a series of ignition sources as it decelerates along the track. The test is considered fail or pass depending upon whether or not a large fuel fed fire results. The "run on" test is more representative of the Lakehurst simulated crash tests (reference 5) conducted by the FAA. The test requires a large apparatus and is relatively expensive to run.

Another intermediate scale flammability test is the wing spillage test described by San Miguel (reference 13) and Salmon (reference 14). Fuel is ejected under pressure from an orifice in the leading edge of a simulated wing against an airstream in a free jet wind tunnel and ignited by a propane torch located underneath the simulated wing. Many parameters such as airspeed, fuel flow rate, orifice diameter and fuel/air temperature could be varied. The criterion used for ascribing a pass or fail to a test was based on the rate of growth of fireballs as they convected downstream through the fuel mist. A fireball radius growth rate of 20 ft/sec or greater during a test was considered to be a fail condition while a value of 10 ft/sec or less was considered to be a pass. These limits were assigned after analyzing a great

15

number of tests and developing a degree of expertise in recognizing their characteristics and potential hazards in a crash situation. The effect of ignition source strength on fireball growth rates was not investigated for a fixed underwing location of the ignition source.

Other small-scale flammability tests are the RAE minitrack, the SWRI spinning disk and the FAA's FCTA tests, all of which provide a relative measure of the fire resistance of various fuel samples on a scale peculiar to the test method.

JPL's flammability test method is based on the flame anchoring phenomenon, which is an important feature of the Lakehurst crash test No. 1 (references 5, 16) It recognizes the fact that a stable flame anchored near the fuel release point following ignition by a transient ignition source poses a particularly dangerous fire hazard in a survivable crash. Factors that influence the flame anchoring phenomenon were studied during one phase of the JPL investigation.

3.2 Description of the Apparatus

The free jet wind tunnel facility used for the flammability tests was a miniature version of the wing spillage facility of Salmon (reference 14). Air was supplied by a centrifugal blower driven by a 50 HP motor. It was passed through screens and a settling chamber before being accelerated by a nozzle contraction. The exit area of the nozzle contraction was 7 in. by 7 in. (17.8 cm x 17.8 cm). A maximum airspeed of 100 m/s (194 knots) could be achieved. The exit airspeed was measured by a pitot-static tube and was controlled by adjusting damper vanes located at the blower entrance.

During initial experiments, a hollow miniwing having a chord of 6 in. (15.2 cm) and a maximum thickness of 1 in. (2.5 cm) was placed symmetrically in the open air jet issuing from the nozzle. Fuel was ejected upwind from an orifice in the leading edge. The orifice diameter could be varied from 1/4 in. to 1 in. (0.6 cm to 2.5 cm) by means of various inserts. Fuel was supplied to the hollow wing by means of a 1 in. dia. stainless steel line from a 15 gal (56.8 liter) pressurized fuel tank. The wing tank pressure was monitored by means of a pressure tap located in the wing tank and connected to a pressure transducer. The output of the pressure transducer was displayed on a strip chart recorder. During a series of tests, the fuel tank pressure was regulated to yield the same wing tank pressure (as monitored on the strip chart recorder), regardless of the flow rate or fuel type used. A fixed wing tank pressure of 1.5 psig was used during all tests reported here. This corresponds to a deceleration of 1 g and a fuel tank width (head) of about 5 ft (1.5 m). By applying Bernoulli's equation this wing tank pressure results in a fuel jet velocity of about 5 m/s.

The fuel jet penetrated 1 to 8 inches (2.5 to 20 cm) upstream into the approaching airstream depending upon the airspeed, before breaking up into droplets and deflecting downwind. Attempts were then made to ignite the droplet-air mixture flowing over the wing by means of a transient or sustained ignition source located directly underneath the wing. The transient ignition source was an electrical spark which discharged approximately 0.067 KW over a

16

duration of about 2 s while the sustained ignition source was an acetylene-air flame of varying intensity. The acetylene torch was ignited by means of the electrical spark during a test. If and when an ignition of the fuel droplet/air mixture was achieved, the acetylene torch was turned off. A key observation during a test was whether a stable, self-supporting flame fed by a freshly generated fuel droplets/air mixture could be established in the wing's wake following ignition either by the spark or by the acetylene torch.

3.3. Results and Discussion

The first series of tests was conducted with airspeed and orifice diameter as the parameters. Baseline flame anchoring data were obtained for Jet A fuel employing a short duration electrical spark as the ignition source. The data are presented in figure 3-1. Notice that at a fixed wing tank pressure (fuel jet velocity) whether or not a stable flame will result depends on the fuel jet diameter and the airspeed. The domains of pass and fail are separated in figure 3-1 by the dashed boundary.

Consider the behavior at a fixed orifice diameter as the airspeed is increased. At very low airspeeds, there is insufficient misting to achieve a spark induced ignition. As the airspeed is increased, the fuel jet begins to breakup into sufficiently fine droplets. Consequently, spark induced ignition of droplet-air mixture is achieved. More importantly, the resulting flame becomes anchored in the wing wake and in some cases envelopes the wing and is continuously fed by fresh droplet-air mixture generated by the disintegrating fuel jet. If the airspeed is increased above a certain value, spark ignition is once again not achieved as the number density of drops becomes too small. Ignition is not possible at any speed for orifice diameter of 1/4 in.

It should be mentioned at this point that similar upstream flame propagation and engulfment phenomenon was observed by Salmon (reference 14) in FAA wing spillage facility during tests with Jet A and underwing ignition. In some cases, flame propagated as far upstream as the fuel jet penetration distance. Motion pictures of this test sequence show remarkable similarity with the events of Lakehurst test No 1.

The flame anchoring tests were next conducted with AMK containing 0.3 percent FM-9 over the same range of airspeeds and jet diameters as employed in tests with Jet A. No ignition could be achieved over the entire test range when the ignition source employed was an electrical spark. An acetylene torch was next employed as the ignition source. The sequence of the test was as follows:

1) The blower was turned on and the airspeed was set at a desired value.

2) The fuel flow was turned on and fuel tank pressure adjusted to give the desired pressure in the wing tank.
3) Ignition was tried with spark source.

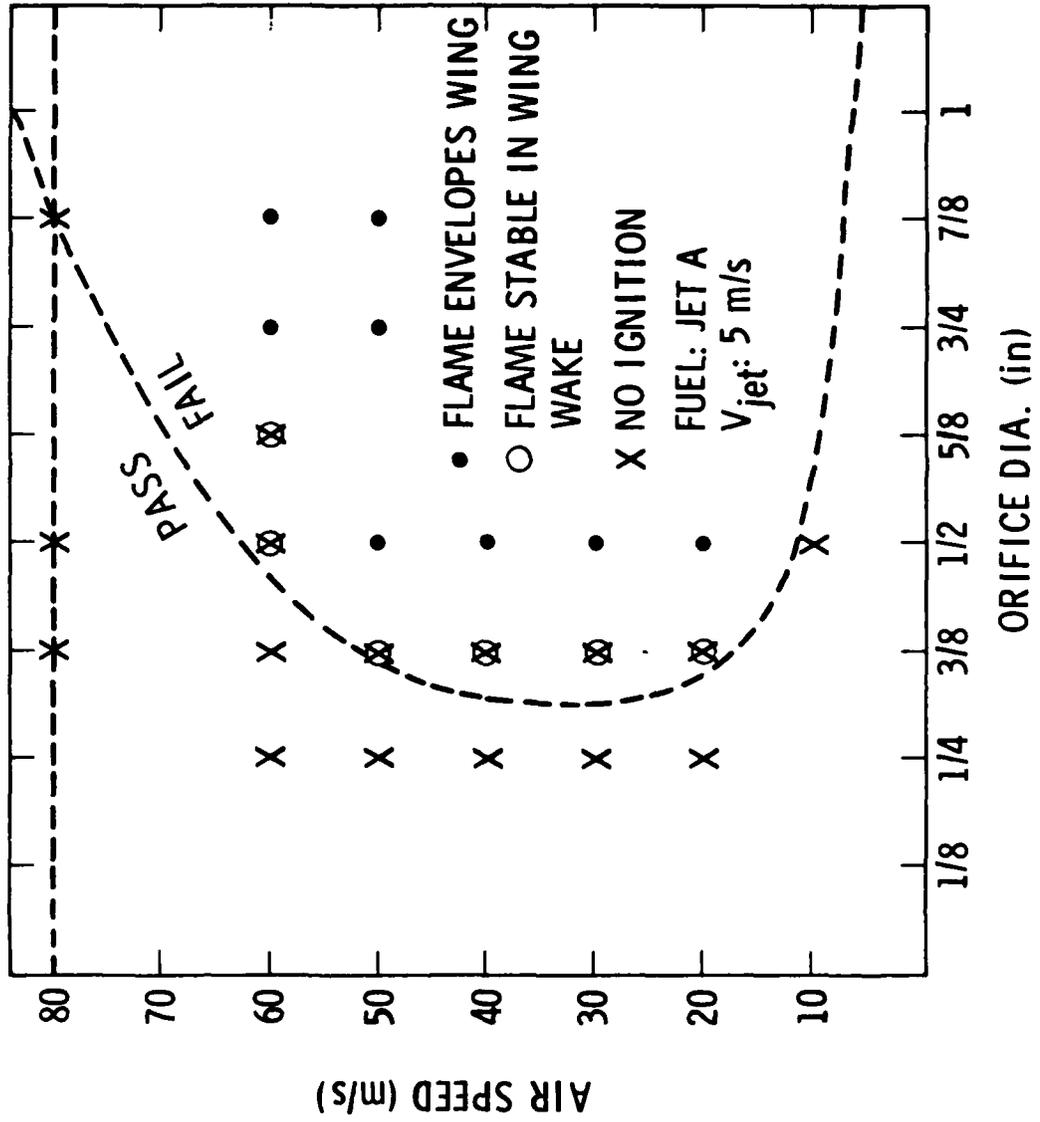4) If unsuccessful, acetylene flow was turned on and torch ignition achieved with spark.

Figure 3-1. Flame Holding Limits for Jet A in Miniwing-shear Apparatus

5) The acetylene-air flame then acted as a continuous ignition source.

Even with the maximum acetylene flow rate employed (0.157 l/s corresponding to heat release rate of 8.8 KW) ignition of virgin AMK containing 0.3 percent FM-9 was not achieved over the entire range of airspeeds and fuel jet diameters employed.

High speed motion pictures (400 frames/s) of the ignition and flame anchoring phenomena were taken during several of the Jet A tests described above. A close examination of these frames revealed that the boundary of the fuel jet after breakup reached the open air jet boundary and it appeared that flame stabilization in many cases may have occurred at the air jet boundary. Thus the shear layer surrounding the air jet acts as a flame stabilizer and incluences the results of these tests. Such a shear layer does not exist in the vicinity of a wing moving through stationary air.

In order to alleviate the above ambiguity in the flame stabilization mechanism, it was then decided to use a bluff body flame holder. The streamlined wing was replaced by a 2 in. diameter cylinder placed with its axis normal to the free-stream direction as shown in figure 3-2. A recirculating flow behind the cylinder created an aerodynamic environment conducive to flame stabilization in its wake as seen in figure 3-3. With fuel ejected from an orifice at the leading edge of the cylinder, a stable, self-supporting flame could be established as seen in figure 3-4, provided the fuel droplet size was sufficiently small. A fixed orifice diameter of 1/2 in. was used in all the tests reported here. A 1.5 psi cylindrical tank pressure resulted in a fuel jet velocity of about 5 m/s or a fuel dump rate of 10 gpm for a 1/2 in. orifice. Three conditions were identified:

1) No ignition of fuel droplets was achieved.

2) Ignition of the fuel droplets was achieved, but the resulting flame was not self-supporting.

3) Ignition of the fuel droplets was achieved and the resulting flame was self-supporting.

The role of the type and intensity of the ignition source in the establishment of the above three conditions will next be discussed.

3.4. Role of Intensity and Type of Ignition Source

The intensity and type of ignition source determines whether ignition of a given droplet-air mixture will occur. If the size and intensity of the ignition source are sufficiently large, ignition of any droplet-air mixture can be accomplished regardless of the droplet size. Thus the transition from condition 1 to condition 2 above is strongly dependent on the ignition source size and intensity. This was obvious from our tests, as the size and intensity of the ignition source was increased from an electrical spark to an acetylene flame of increasing heat release rate. In many instances, ignition was not achieved with a spark source and not achieved even with an acetylene
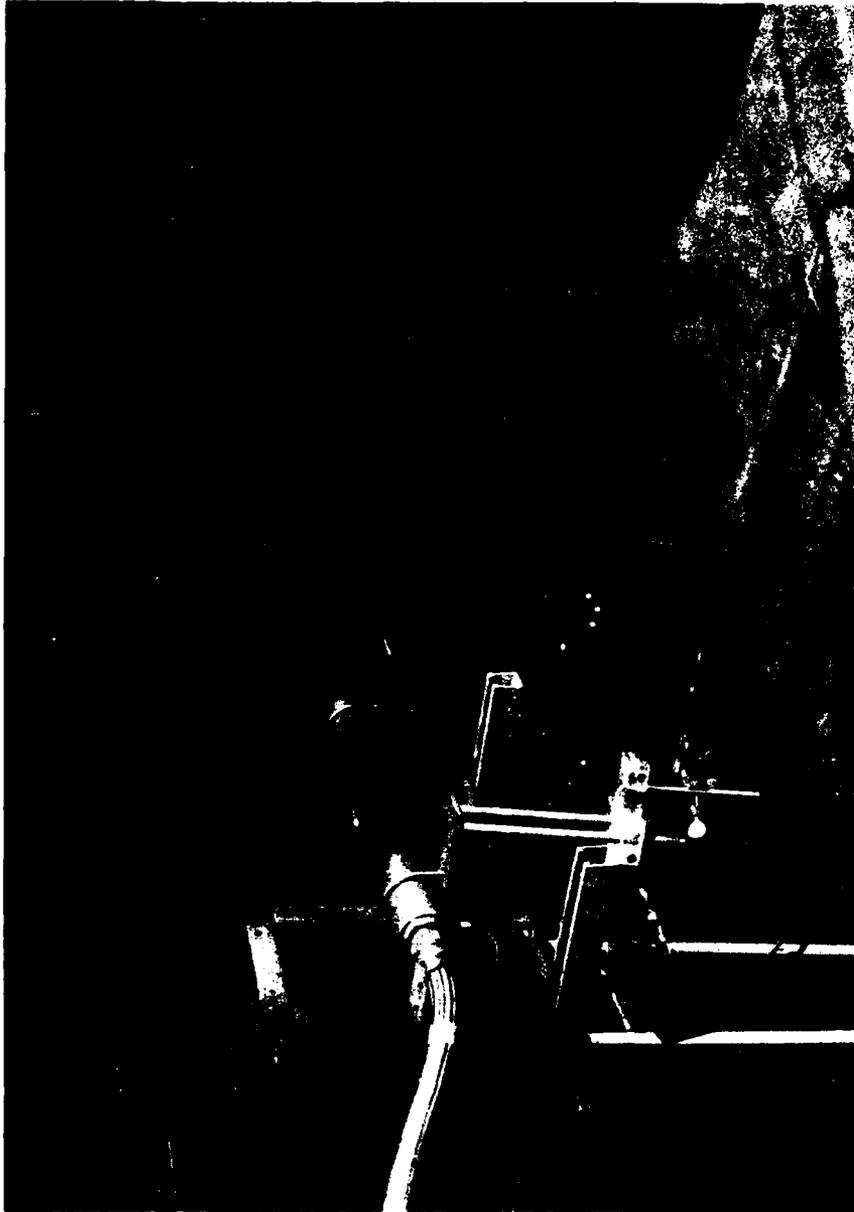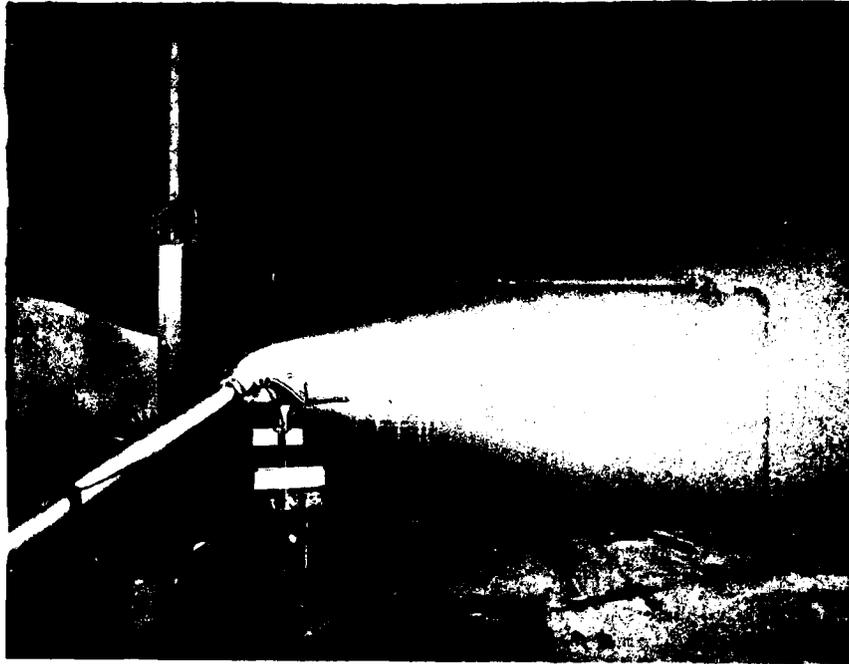
19

Figure 3-2. Apparatus for Cylinder Flame Holding Tests

20
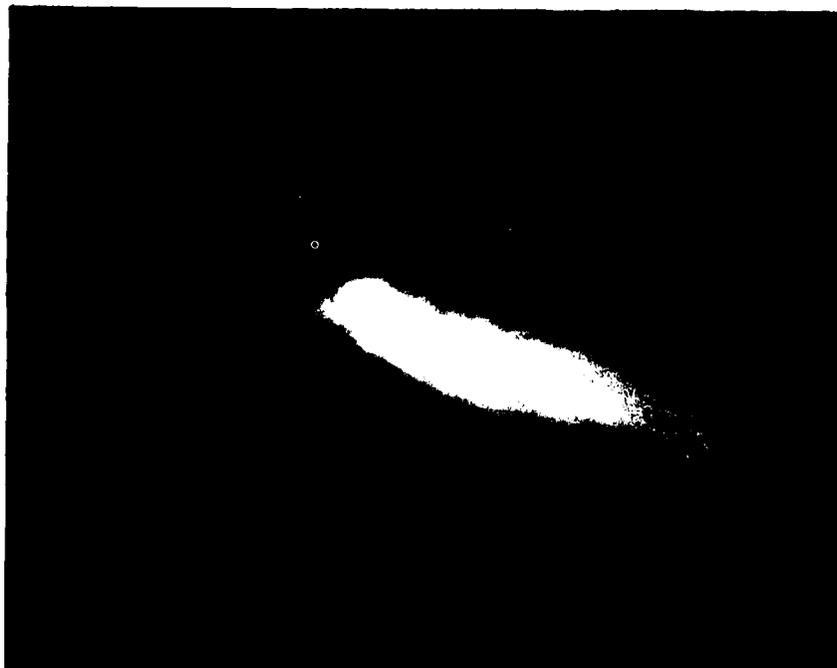
Figure 3-3. Fuel Jet Breakup in Flame Holding Experiments

Figure 3-4. Flame Anchoring at U_∞ = 50 m/s, FR = 4.65

flame below a certain acetylene flow rate. However, when the acetylene flow rate was increased above a certain value, heat release rate in the acetylene flame was sufficient to ignite the droplet-air mixture. This is also evident from large-scale tests. For example in Lakehurst test No. 5, the fuselage mounted hot rocket exhaust torches have sufficient intensity to cause the ignition of the 0.3 percent FM-9 droplet-air mixture. The same mixture, however, was not ignited by the ignition sources (smudge pots) located on the ground (reference 16).

The point then is, provided the ignition source is large enough, no fuel is immune from ignition. The crucial test should be whether condition 3 above is satisfied. That is, after ignition of the droplet-air mixture is accomplished and the ignition source is shut off, will the fire be self-supporting? It is evident from a study of Lakehurst test No. 1 and 5 that if the resulting flame is self-supporting, it leads to disasterous results; if it is not self-supporting, a large-scale fuel fire is prevented.

It is obvious that in a transition from condition 2 to condition 3 above, the size and intensity of the ignition source are not important. Only the droplet size (degree of misting) and aerodynamic factors are important. The philosophy behind cylinder flame holding tests was 1) to deliberately provide an aerodynamic environment that would ensure flame stabilization and 2) to provide an ignition source large enough to achieve ignition of a given droplet-air mixture. Whether condition 3 above is then achieved or not depends entirely on the degree of misting, which in turn, is governed by the airspeed and rheological properties of the fuel.

As was found during the miniwing tests, no ignition of 0.3 percent FM-9 AMK could be achieved over the entire airspeed range (20 to 80 m/s) during the cylinder flame anchoring tests even with the highest acetylene flow rate (0.157 l/s corresponding to a heat release rate of 8.8 KW) in the ignition torch. It was then decided to use degraded AMK fuel in the tests to determine the pass/fail boundary as a function of airspeed and the degree of degradation.

A good measure of the degree of degradation of a given AMK fuel is the filter ratio as determined by a test described in appendix C. Test samples of progressively lower filter ratios were prepared by degrading the virgin AMK fuel by means of repeated passes through a centrifugal pump. The filter ratio was measured before the start of each flammability test. As mentioned earlier, during all the tests the wing tank pressure was maintained at 1.5 psig while a fixed orifice diameter of 0.5 in. was used. Tests were run for 9 different values of the filter ratio and for airspeeds in the range 20 to 80 m/s (39-156 knots). The pass/fail criterion used was to designate a test a fail if condition 3 discussed above was achieved, i.e., if a self-sustained flame anchored in the cylinder wake was established following ignition by a transient acetylene flame. The test was designated a pass if 1) no ignition was achieved or, 2) ignition was achieved, but the resulting flame was not self-sustaining.

The data are presented in figure 3-5. Conditions 1, 2 and 3 discussed above are represented respectively, by symbols O, ⊗ and X. A pass/fail boundary which separates X's from ⊗'s and O's is also shown. It may be seen
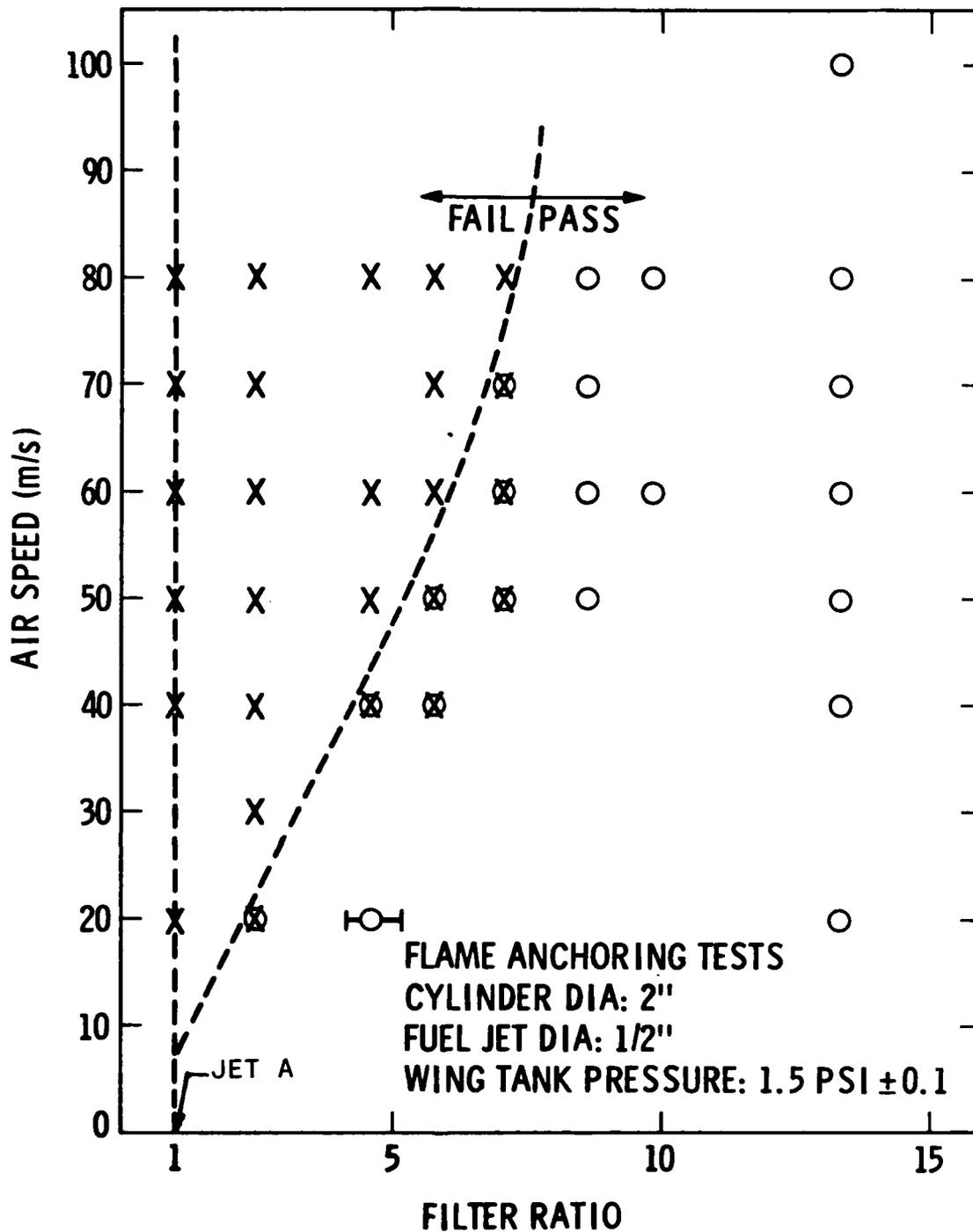
22

Figure 3-5 Pass/Fail Boundary for Degraded AMK(0.3 percent FM-9)
in Cylinder Flame Anchoring Experiments.
Ignition Source: Acetylene-Air Flame, 8.8 KW

that for filter ratios greater than about 7, a self-sustaining flame anchored in the cylinder wake could not be established up to an airspeed of 80 m/s (156 knots). At filter ratios lower than 7, there was a critical airspeed above which the misting was sufficient to sustain a flame anchored in the cylinder wake and below which misting was insufficient to sustain such a flame. This critical airspeed has a value below 20 m/s for Jet A and it increases as the filter ratio is increased.

The effect of ignition source intensity on the ignition characteristics of flowing droplet-air mixtures is shown in figure 3-6. The results are presented for a fixed airspeed of 50 m/s. As the fuel filter ratio is increased, presumably the droplet SMD increases also, while the aerodynamic parameters remain unchanged. It may be seen that ignition source intensity required to achieve ignition of the droplet-air mixture increases as the fuel filter ratio is increased. For pure Jet A (FR = 1), intensity of even an electrical spark (0.067 KW) is sufficient to cause ignition. The next three levels of intensity were provided by an acetylene flame whose acetylene flow rate was measured and controlled. The dashed curve shows the threshold intensity required to achieve an ignition of a given filter ratio fuel under the prescribed conditions of the experiment. It may also be seen from this curve that, provided the intensity of the ignition source is high enough, any fuel may be ignited. However, after the ignition is achieved and the ignition source turned off, only fuels with filter ratio less than about 7 resulted in self-sustained flame as discussed previously in reference to figure 3-5.

The question now arises as to what is the influence of increased fuel dump rate and of ignition source intensity significantly higher than that employed in the foregoing investigation. Conceivably, a large ignition source in conjunction with a large fuel dump rate could initially set up a large fuel fire, which would have enough heat release rate to be self-supporting after the ignition source was turned off. Thus, the pass/fail boundary based on the flame anchoring criterion as shown in figure 3-5 would become dependent on the ignition source intensity. To see if this was the case, preliminary experiments were conducted with FR = 10 fuel after two modifications to the existing apparatus:

1. The fuel dump rate was increased by a factor of 4 to 40 gpm using a 1 in. orifice at the leading edge of the cylinder.

2. The ignition source intensity was increased by a factor of about 10 to 90 kW by increasing the acetylene flow rate to 1.6 l/s. Also the flame was made hotter by premixing the acetylene with oxygen rather than employing an acetylene diffusion flame in air as was done previously.

With these modifications, the ignition source was now intense enough to ignite even virgin AMK in the facility at air speeds as low as 40 m/s.

When tests were run with FR = 10 fuel, the powerful new ignition source set up a fuel fire 12 to 15 ft. long in the wake of the cylinder. However, this fire persisted only as long as the ignition source was on. As soon as the ignition source was turned off, the fire could no longer be supported even though fuel continued spillage from the leading edge of the cylinder. This was found to be the case for the entire airspeed range up to 80 m/s. These
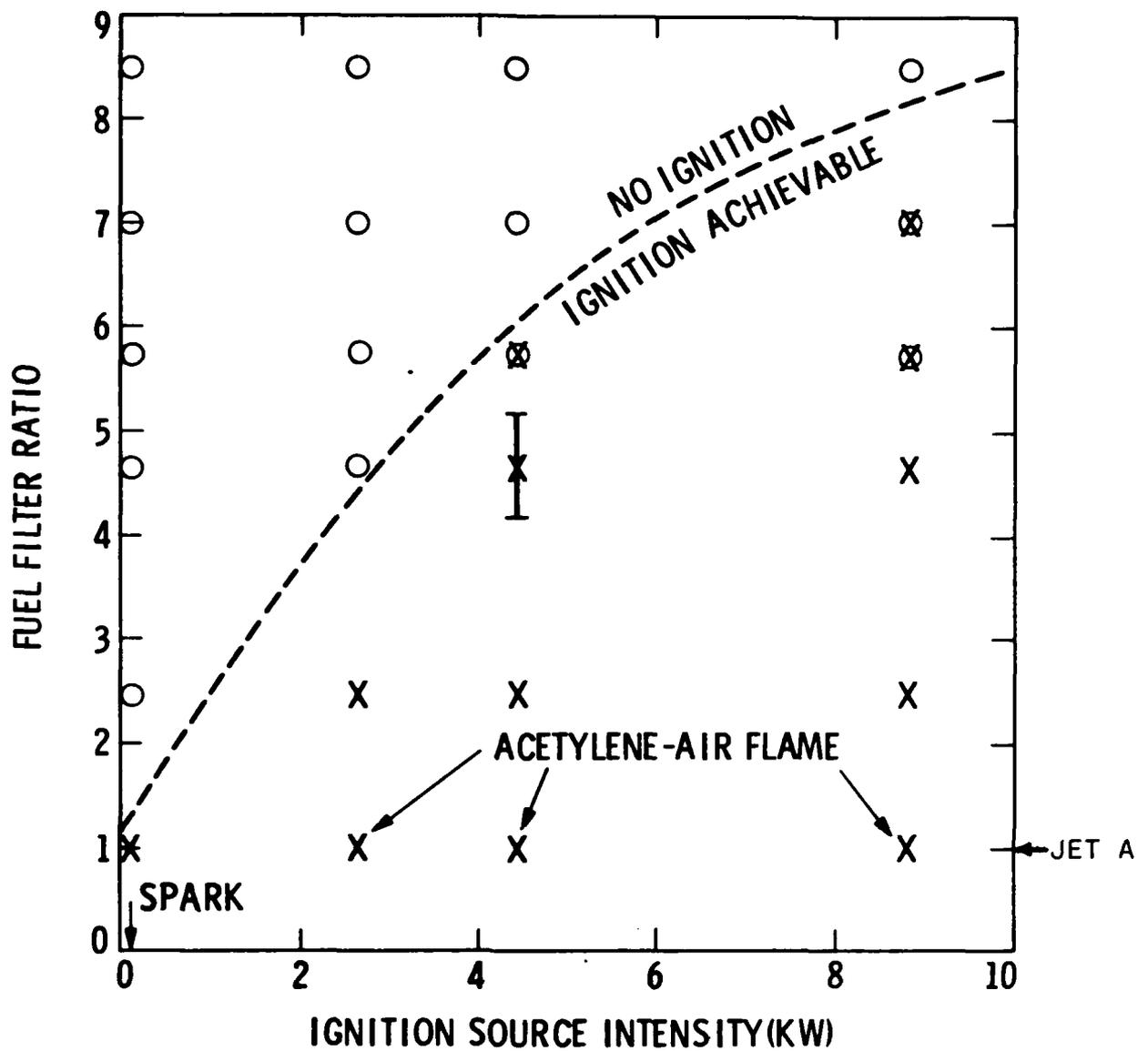
24

Figure 3-6 Threshold Ignition Source Intensity as a Function of Filter Ratio for Degraded AMK(0.3 percent FM-9) U_∞ =50 m/s

tests suggest that the pass/fail boundary based on the flame anchoring criterion as shown in figure 3-5 is apparently not dependent on the intensity of the ignition source employed--at least over the wide range of intensities employed in the present investigation.

It should be emphasized that fuel dump rates in actual crash situations may be two to three orders of magnitude larger than those employed in the present laboratory scale experiments. The intensities of ignition sources such as torching engines ingesting fuel could also be much larger. To develop a greater degree of confidence in flame anchoring criterion and to demonstrate that it is indeed independent of the ignition source intensity, experiments at a scale much larger than that of the experiments reported here are needed.

3.5 Conclusions

1.   Self-sustained flame anchoring in the wake of a bluff body with upstream ejection of fuel was found to be dependent upon free-stream air speed and fuel rheological properties. A new pass/fail criterion based on this flame anchoring phenomenon has been proposed.

2.   In the present experiments employing and fuel dump rate of 10 gpm, no self-supporting flame anchored in the wake of a cylinder could be established for filter ratios greater than 8 and airspeeds up to 80 m/s (156 knots).

3.   Preliminary investigation of increased fuel dump rate and significantly larger ignition source intensity suggests that the pass/fail boundary using the flame anchoring criterion is not significantly altered over a wide range of these two parameters in the present laboratory scale experiments.

4.   The intensity of ignition source plays a key role in determining whether or not ignition of a given droplet-air mixture can be achieved. However, over the wide range of ignition source intensities (0.067 to 90 kW) used in the present investigation, whether the resulting flame is self-supporting or not depends only on fuel misting and aerodynamics.

4. FLAME SPREAD ON THE SURFACE OF A LIQUID FUEL POOL

4.1. Background

As was discussed in chapter 1, the phenomenon of flame spread on the free surface of a liquid fuel pool is of considerable interest in the study of postcrash fire scenario. The rate of flame spread determines the rate of growth of fire intensity and hence the time available for safe evacuation of survivors.

Conventional aviation turbine fuels have flash point temperatures well above typical wing tank temperatures. Consequently, the flame spread rates over the surface of such fuels are much lower than those over the surface of low flash point fuels such as gasoline. For the latter type of fuels, a combustible mixture of fuel vapors and air already exists close to the free surface even at moderate to low ambient temperatures (0 to 30° C). Previous investigations of flame spread over the surface of high flash point fuels have shown that the principal mechanism of flame spread is convective heat transfer to the liquid fuel ahead of the flame front. Viscosity plays a key role in convective heat transfer through the liquid layer. Therefore, antimisting fuel additives, which essentially alter the rheological properties of the fuel may be expected to have influence on the flame spread rate over the liquid surface. The present investigation was undertaken to assess this influence. Flame spread rate measurements were carried out with the depth of the fuel layer as a parameter for both Jet A and AMK fuel containing 0.3% FM-9 additive. Initial fuel temperature is expected to have a strong effect on the flame spread rate. However, in the preliminary investigation conducted here, the effect of initial fuel temperature on the flame spread rate was not investigated systematically and all experiments were conducted at nearly the same initial temperature. The effect of the presence of a porous substrate on flame spread was also investigated.

4.2. Apparatus and Procedure

The apparatus consisted of a tray, 6 ft. long x 6 in. wide x 1 in. deep, fabricated from 1/8 in. stainless steel plate. The tray was welded onto an angle iron frame. Ten thermocouples, fabricated from 28 ga. chromel-alumel wire were placed six inches apart along the length of the tray. The thermocouples were supported by 1/8 in. stainless steel tubing which was inserted from the tray bottom through swagelok fittings. The swagelok fittings provided a leakproof seal around the 1/8 in. tubing, while enabling an adjustment of the junction height above the surface of the liquid fuel. During all the tests, the junction height was adjusted at 1/8 in. above the free surface for all thermocouples. A photograph of the instrumented tray used in the flame spread experiments is shown in figure 4-1.

The lead wires from the thermocouples were connected to a selector switch, which at a given position, connected the output of one of the thermocouples to a strip chart recorder. During operation, the selector switch was manually stepped progressively through the ten positions while monitoring the output at the strip chart recorder. When the temperature of a thermocouple being monitored rose above a certain level, the selector switch
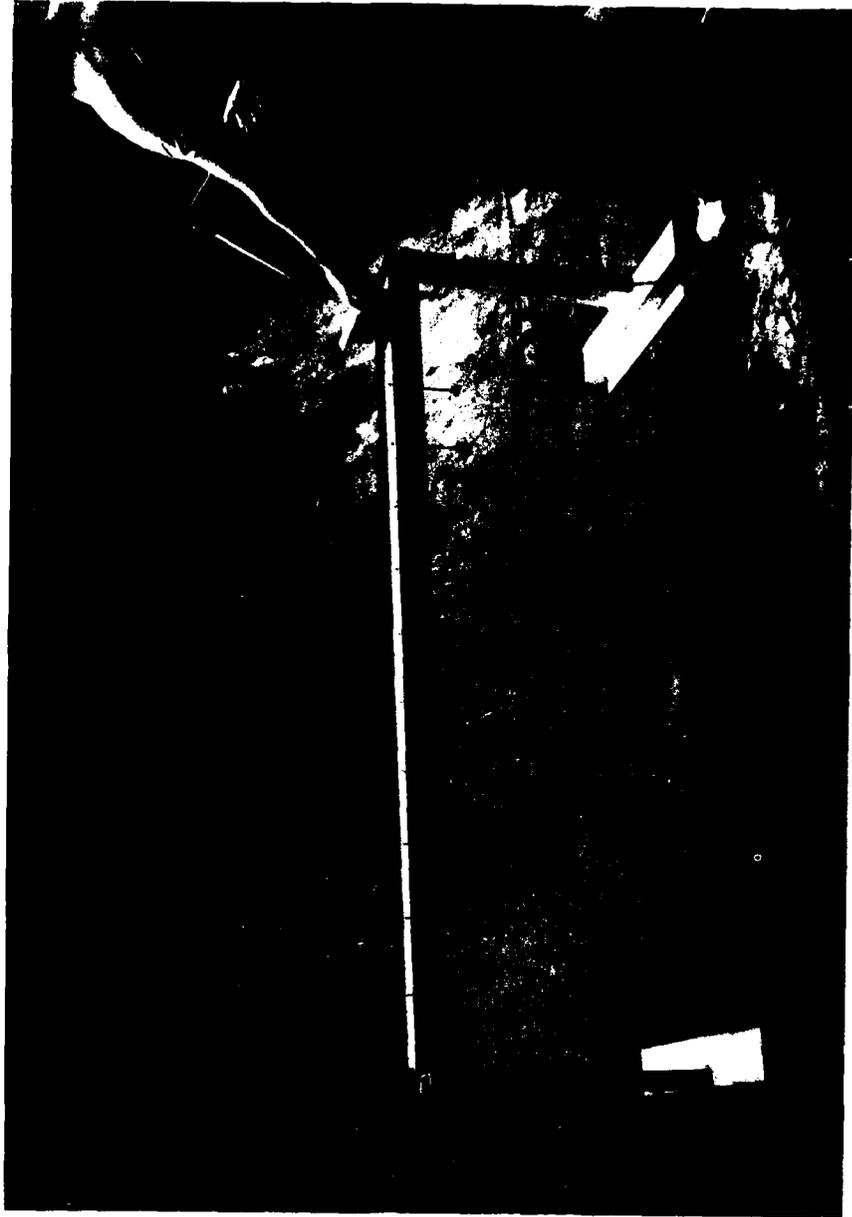
Figure 4-1. Apparatus for Flame Spread Tests

was stepped to the next thermocouple position. The flame spread rate was slow enough so that this could be accomplished manually. A series of flame photographs is shown in figure 4-2 for different times during the flame spread process. Due to the fluctuations in the position of the flame front, combined with the finite response time of the thermocouples, the response at the strip chart recorder showed some fluctuations superimposed on an orderly temperature rise. During data reduction, a smooth curve was visually drawn through each temperature record to determine the time at which the response crossed a certain threshold temperature. The data were then plotted on an x-t diagram and the flame spread rate was determined therefrom by fitting a straight line through the data points. A sample strip chart record and the corresponding x-t diagram are shown in figure 4-3. Three test runs were conducted under identical conditions (fuel layer depth, fuel type) to check the repeatability of flame spread rate and to estimate uncertainty in the measurement.

At the beginning of each run, the tray was filled with fuel to a desired height. The tray was carefully leveled using spirit levels to ensure nearly uniform depth along the length of the tray. Due to warpage of the tray bottom during welding a variation of ±1/16 in. in the measured depth of the liquid layer was introduced. To achieve a uniform depth of the fuel layer, previous experiments by McKinven et al. (reference 6) utilized a water substrate underneath the fuel layer. This technique could not be used in the present experiments due to the coagulation of the polymer additive upon contact with water. The thermocouple heights were then adjusted so that the junction protruded 1/8 in. above the liquid free surface. The initial air and fuel temperatures were recorded. An approximately 6 in. length of the tray from one end was then partitioned by means of a removable metal plate and the fuel in this compartment was ignited by means of an acetylene torch. Ignition was not achieved instantly, but required heating the fuel to a temperature above the flash point. Once the entire surface of the 6 in. compartment had been ignited, the metal plate partition was carefully removed (so that no waves were set up) and the flame was allowed to spread along the remaining free surface of the tray. The first thermocouple was encountered six inches down the tray axis from the initial flame front position after the partition was removed. When the flame had propagated the entire length of the tray, it was extinguished by means of a tray cover (figure 4-2) which cut off the air entrainment into the fire. The tray was then drained, washed and cooled with water and wiped clean to prepare for the next run. Five different fuel depths were used: 1/8 in., 1/4 in., 3/8 in., 1/2 in. and 3/4 in. For fuel depths less than 1/3 in., it was not possible to maintain the flame--heat loss to the metal tray quenched the flame. A similar observation was made by McKinven et al. (reference 6).

A pair of tests were run to investigate flame spread on a porous substrate soaked with Jet A and AMK. During these tests, the tray was filled with a 1/2 in. layer of sand carefully packed and leveled with a flat surface. Fuel was poured over the sand until the substrate was saturated. Excess liquid on top of the sand layer was blotted off by means of absorbent tissue paper. Ignition was accomplished in the same manner as in the pure liquid layer experiments. It was found that the flame nearly failed to spread initially in the porous substrate experiments and continued burning locally for a considerable length of time. The localized fire was fed by fuel that seeped through the porous substrate. Eventually, however, due to conduction
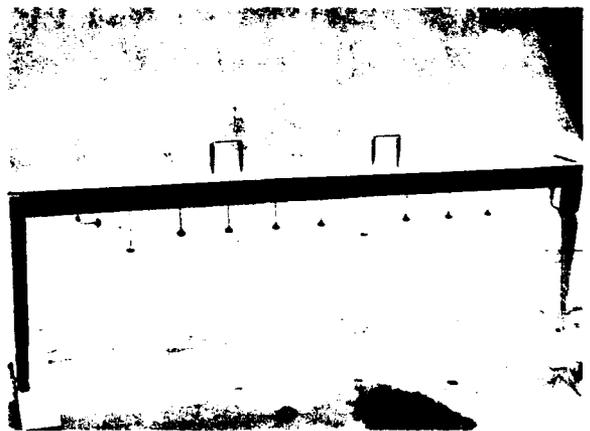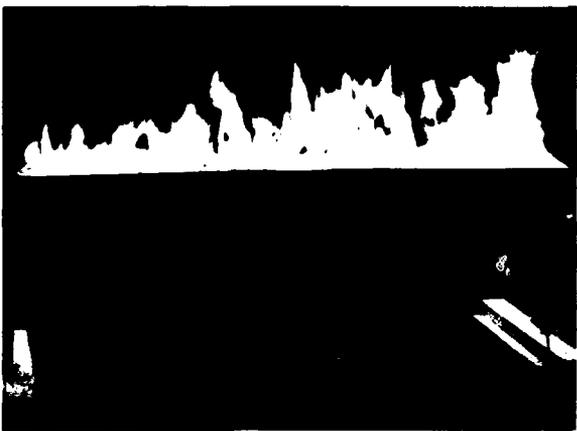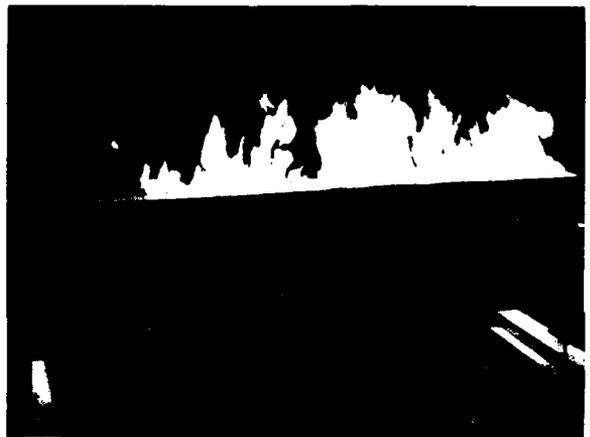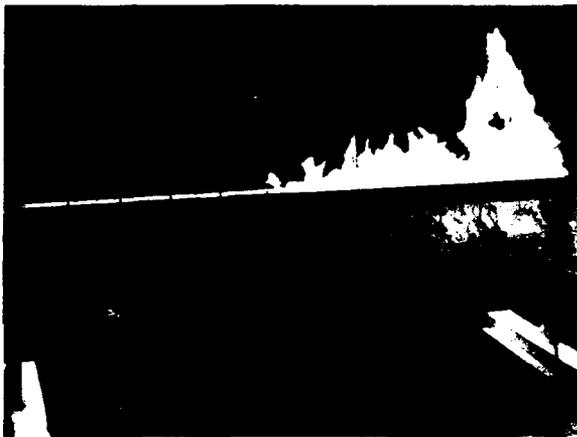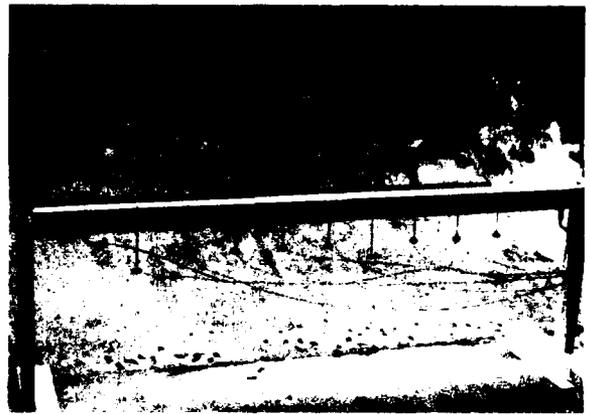
29

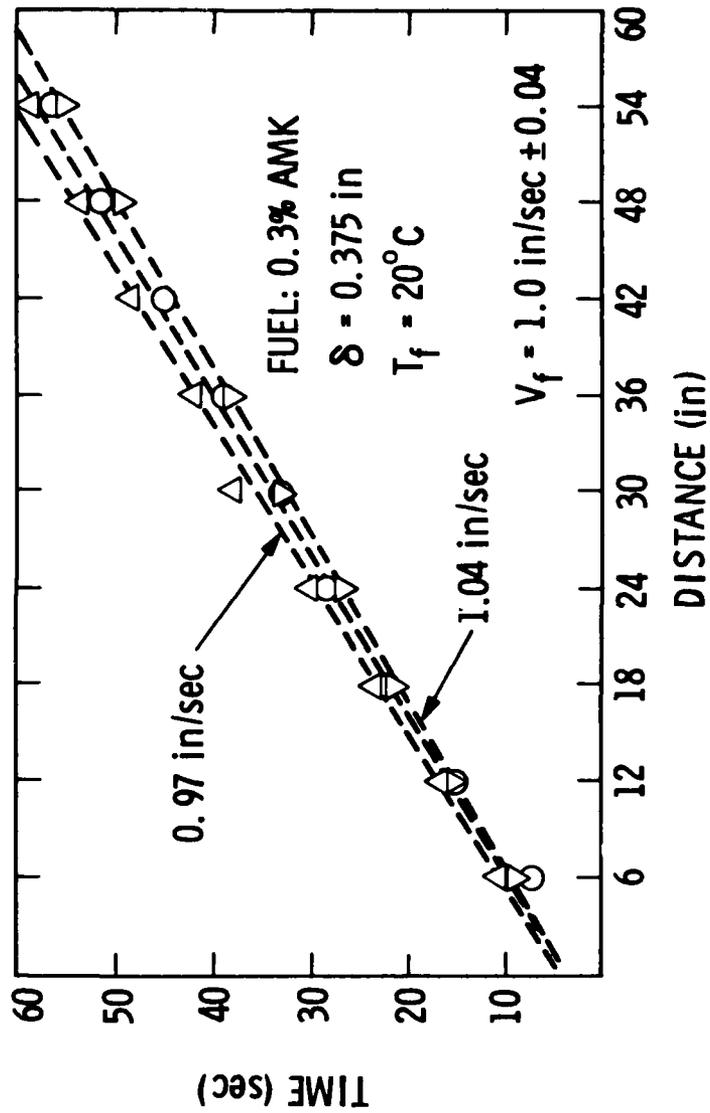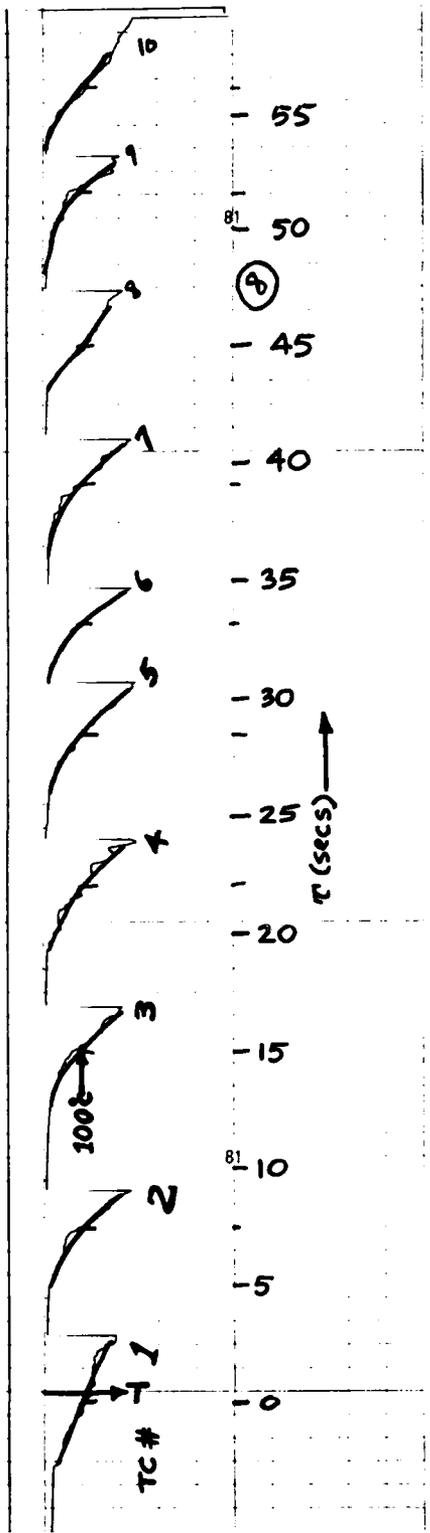Figure 4-2. Sequence Showing Progression of Flame Along
the Fuel Tray

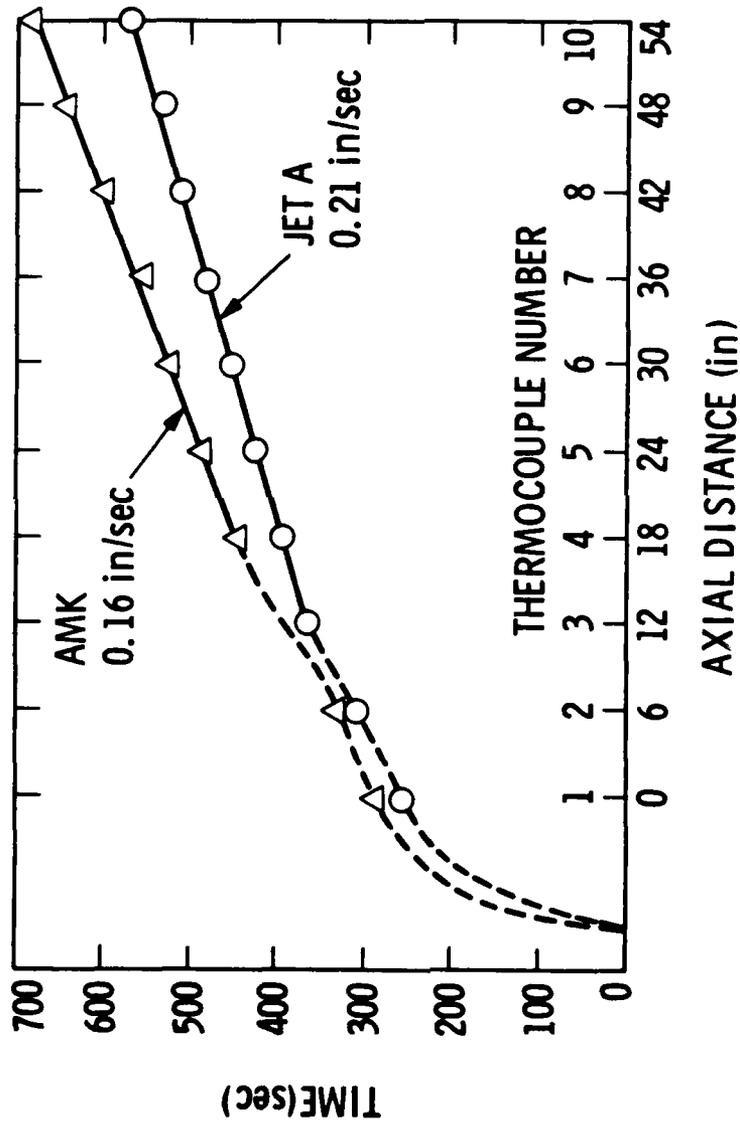Figure 4-3. Sample Strip Chart Record and x-t Diagram for Flame Spread Tests

FUEL: 0.3% AMK
$\delta = 0.375$ in
$T_f = 20°C$

$V_f = 1.0$ in/sec ± 0.04

0.97 in/sec

1.04 in/sec

Figure 4-4. x-t Diagram for Porous Substrate Experiments

32

along the tray and radiation from the flame a slow spread began. The x-t diagrams for porous substrate experiments are shown in figure 4-4.

4.3 Results and Discussion

Flame spread rate data are plotted in figure 4-5 as a function of the liquid layer depth for Jet A and AMK containing 0.3 percent FM-9. In general the spread rate increases as the layer depth is increased. Within the uncertainty of the data, no significant differences between flame spread rate over Jet A and AMK fuel could be discerned.

The increase in the flame spread rate with fuel layer depth was most noticeable in the range 3/8 in. < < 3/4 in. For δ < 3/8 in., the trend was somewhat erratic. This may be caused by the increasing role of conduction along the tray material as the fuel layer depth is decreased. At small depths, convection currents are suppressed but heating of the fuel ahead of the flame front is enhanced by conduction along the metal tray. At fuel layer depths less than 1/8", the rate of heat loss to the tray is sufficient to quench the flame. Similar observation was reported by McKinven et al. (reference 6). The reason for increasing flame spread rate with increasing fuel layer depth was explained qualitatively by Makinven et. al (reference 6) as progressive reduction in viscous damping of surface currents by the tray bottom as the fuel layer depth is increased.

Also shown on Fig. 4-5 are the data of Eklund (reference 15) for Jet A and AMK containing 0.4% FM-4 additive. The flame spread rate measured by Eklund (reference 15) for Jet A is somewhat higher than that measured in the present investigation. This difference could be due to differences in the fuel composition (which affects flash point temperature), experimental apparatus and techniques used for spread rate measurement. The noticeable difference in the flame spread rate behavior between Jet A and AMK was not observed in the present experiments.

During experiments with a porous substrate, the initial spread rate of the flame was very slow following ignition by means of a propane torch. Initially the flame continued to burn almost locally with very little spread. However, as it began to grow in intensity, the radiation from the flame and conduction along the tray wall contributed to heating of the fuel ahead of the flame and spread rate increased. After some time the spread rate achieved a steady value (see Fig. 4-4) which was still 1/5 to 1/6 of the measured spread rate for a fuel layer in the absence of a porous substrate. The measured steady value of flame spread rate over a porous substrate was slightly lower for AMK (0.16 in/s) than for Jet A (0.21 in/s).

4.4 Conclusions

1. Within the uncertainty of the present data, no significant difference between the flame spread rate over pools of Jet A and AMK fuels was observed.
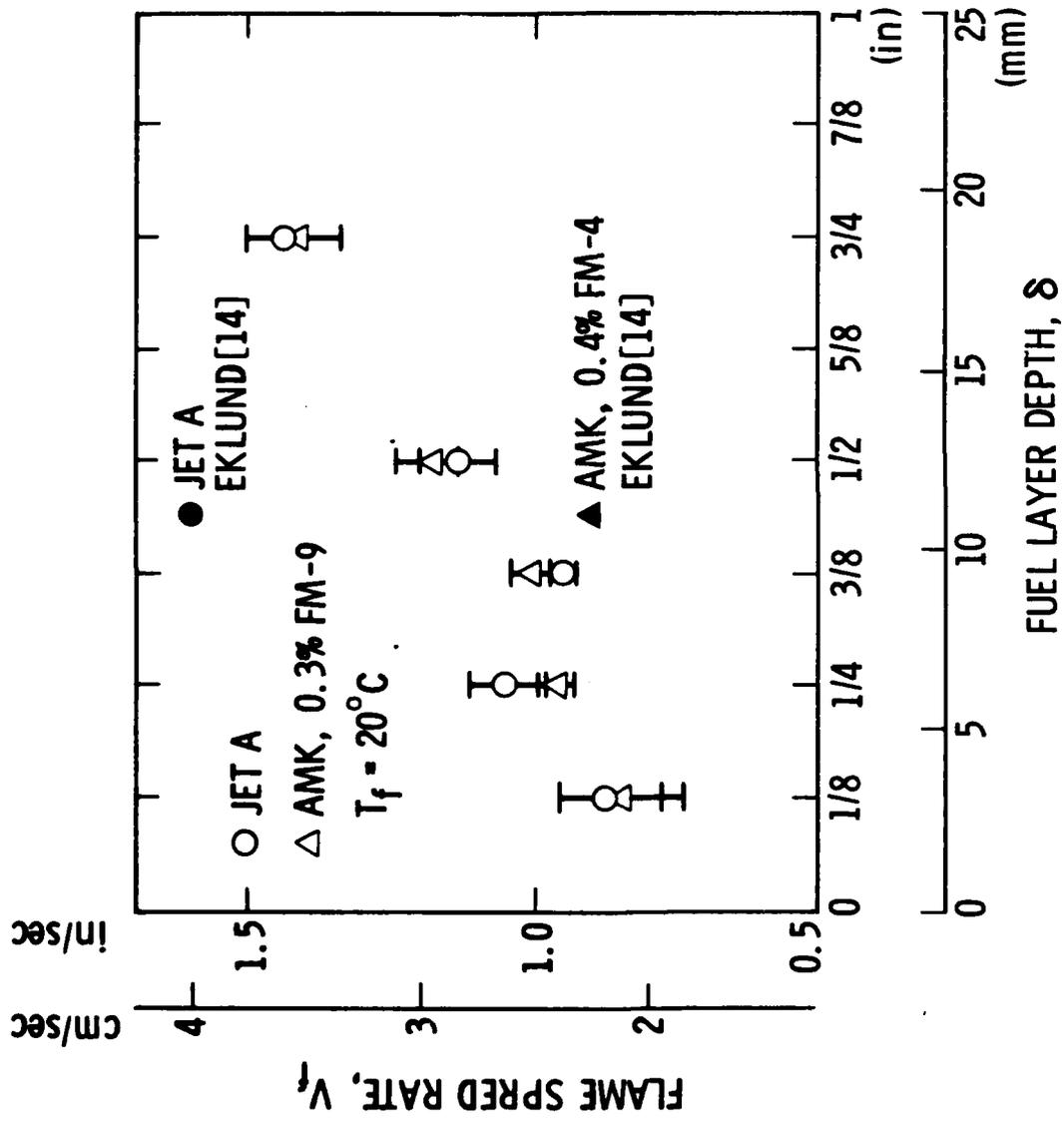
Figure 4-5. Flame Spread Rate Data as a Function of Fuel Layer Depth

2.   Over the range of fuel layer depths (δ) tested (1/8 to 3/4 inch),
flame spread rate generally increased with increasing δ from about 2 cm/sec to
3.5 cm/sec.

3.   The presence of a porous substrate inhibits flame spread.
Steady-state flame spread rate over a porous substrate soaked with fuel (Jet A
or AMK) was 1/5 to 1/6 of the measured spread rate in the absence of the
porous substrate.

REFERENCES

1. Botteri, B.P. et al.: Aircraft Fire Safety Vol. 2. AGARD Advisory
   Report No. 132. November (1979).

2. Enders, J. H. and E. C. Wood: Special Aviation Fire and Explosion
   Reduction (SAFER) Advisory Committee Final Report, Vol. 1. Report
   FAA-ASF-80-4. June (1980).

3. U. S. Air Carrier Accidents Involving Fire 1965 through 1974 and Factors
   Affecting the Statistics. Report No. NTSB-AAS-77-1. February (1977).

4. National Transportation Safety Board, Aircraft Accident Reports.
   Periodic.

5. Zagarella, A.: Lakehurst Full-Scale Aircraft Crash Tests of Antimisting
   Kerosene. NAVAIRENGCEN Test Letter Report No. NAEC-TR-183. Aug. (1980).

6. Mackinven, R. et al.: Influence of Laboratory Parameters on Flame
   Spread Across Liquid Fuels. Combustion Science and Technology, Vol. 1
   pp. 293-306 (1970).

7. Fleeter, R., Petersen, R. A., Toaz, R. D., Jakub, A. and Sarohia, V.
   (1981) "Antimisting Kerosene Atomization and Flammability". Interim
   Report, U.S. Department of Transportation, Federal Aviation
   Administration.

8. Fleeter, R., Toaz, R. D. and Sarohia, V. (1982) "Application of Digital
   Image Analysis Techniques to Antimisting Fuel Spray Characterization".
   Paper accepted for presentation at the ASME Winter Annual Meeting,
   Phoenix, AZ, November 1982.

9. Fleeter, R., Parikh, P. and Sarohia, V. (1982) "Antimisting Kerosene
   Atomization and Combustion Performance". Report to the U.S. Department
   of Transportation, Federal Aviation Administration (in press).

10. Glassman, I. (1977) "Combustion". Academic Press, New York.

11. Faeth, G. M. and Lazar, R. S. (1971) AIAA J. 9, 2165.

12. Miller, R.E. and S. P. Wilford: Simulated Crash Fire Tests as a Means of
    Rating Aircraft Safety Fuels. Royal Aircraft Establishment Report No.
    71130 May (1971).

13. San Miguel, A.: Antimisting Fuel Kinematics Related to Aircraft Crash
    Landings. Journal of Aircraft. AIAA, (1979).

14. Salmon, R. F.: Wing Spillage Tests Using Antimisting Fuel. Federal
    Aviation Administration Report No. FAA-CT-81-11. February (1981).

15. Eklund, T. I.: The Effect of Polymeric Additives on Fire Spread Across
    Turbine Fuel. Combustion Science and Technology, Vol. 17. pp. 73-74
    (1977).

16. Private Communication with R. F. Salmon, FAA Tech. Center.

APPENDIX A.

Quantitative Measurement of Flammability in the Miniwing Shear Apparatus

It is inherent to flammability testing that some intrinsic empiricism exists. As long as this is recognized and experimental repeatibility is established, it is good experimental practice to use and rely on such heuristic data. An example of this approach within the AMK program is the use of the filter ratio (FR) as a measure of fuel degradation. The FR is defined as the time for a specific quantity of AMK contained in a vertically oriented, specifically designed container to pass through a particular filter under gravity, divided by the time for the same quantity of Jet A to do likewise. This test is highly precise (repeatibility is high) and has found wide acceptance in the program despite the fact that it is completely heuristic and gives no information on the physical state of the polymeric solution it attempts to analyze.

In the case of flammability testing, the temperature along the jet centerline was measured with thermocouples of relatively slow response time (~0.10 s). The time-averaged maximum temperature along the jet axis is resolved and used as a measure of fuel flammability. No claim is made about the relationship of such a measure to specific physical data on fuel mist combustion except to rely on the observation that as a greater fraction of the fuel present in the mist is burned, the peak axial temperature increases. Similarly, we say that as the antimisting polymer is degraded, the FR decreases and hence conclude that FR is a measure of degradation. This peak temperature is corrected for the gross influence of changes in the fuel and air flows. As an example, identical experimental conditions (except for a doubling of the fuel injection rate) yield roughly a doubling of the observed temperature. This is felt simply to reflect the change in the amount of fuel present and not a fundamental change in fuel atomization or mist flammability. For these reasons a reduced temperature, θ, was derived (see Appendix of Fleeter et al. 1981) as

$$\theta = \frac{\Delta T \; C_p \; \dot{M}_a}{\dot{M}_f \; q_f} = \frac{\dot{m}_f \; q_f}{\dot{M}_f \; q_f} = \frac{\dot{m}_f}{\dot{M}_f}$$

where ΔT is the measured temperature rise, C_p is the (assumed constant) specific heat of air, $\dot{M}_a$, and $\dot{M}_f$ are the air and fuel mass flow rates respectively, $\dot{m}_f$ is the fuel consumption rate due to combustion, and q_f is the amount of heat released per unit mass of fuel consumed. Flammability results are all expressed in terms of this variable. While its value may be influenced by such factors as air entrainment and temperature distribution variation in the radial direction, the repeatibility of the measure is well established (Fleeter et al. [reference 7]). Further, combustion of Jet A exhibiting a large fireball and leaving little residue except for considerable carbon soot typically yields values of θ of about 0.6. Taken literally this implies that 60% of the fuel was burned to completion (H_2O and CO_2 as the only products of combustion). In contrast, several tests with AMK yielded values of θ around 0.01, indicating 1% of the fuel took part in combustion. This was accompanied with observation of large amounts of fuel residue in the form of liquid deposited on the facility walls and floor with a relatively small flame.

APPENDIX B

Interpretation of Flammability Behavior as a Result of Classical Drop Combustion Behavior

The fact that stationary, spherical drops of fuel burn according to the relation

$$\partial(D^2)/\partial t = C_1 \tag{1}$$

where D is the drop diameter, t is time and C_1 is a constant is well established both theoretically (e.g., Glassman, [reference 10]) and experimentally (e.g., Faeth and Lazar, [reference 11]). Integration of (1) yields the relation

$$D^2 = C_1 t + C_2 \tag{2}$$

$$\text{or} \qquad D^3 = (C_1 t + C_2)^{3/2}. \tag{3}$$

The rate of fuel consumption by combustion, $\dot{m}_f$, is directly equated to this volume change

$$\dot{m}_{f,i} = \frac{\pi}{6} \rho f \frac{\partial (D_i^3)}{\partial t} = \frac{\pi}{4} \rho f \, C_1 \, (C_1 t + C_2)^{1/2} \tag{4}$$

Further, equation (2) implies that

$$D = (C_1 t + C_2)^{1/2} \tag{5}$$

so that

$$\dot{m}_{f,i} = \frac{\pi}{4} \rho f \, C_1 \, D_i \tag{6}$$

Thus the rate of fuel combustion is proportional to the drop diameter.

The reduced temperature, θ, is by definition directly proportional to $\dot{m}_f$. The total fuel consumption rate $\dot{m}_f$ may be related to the individual drop combustion rates $\dot{m}_{f,i}$ by

$$\dot{m}_f = \sum_i \dot{m}_{f,i} = \frac{\pi}{4} C_1 \, \rho f \sum_i D_i \tag{7}$$

Since the total fuel flux $\dot{M}_f$ into the spray is not a function of how finely the spray is atomized, the total mass of drops must be conserved.

$$\text{i.e.,} \qquad \rho f \sum_i \frac{\pi}{6} D_i^3 = \dot{M}_f \tag{8}$$

38

Thus from equations (7) and (8) we conclude

$$\epsilon = \frac{\dot{m}_f}{\bar{M}_f} = \frac{\frac{\pi}{4} C_1 \rho_f \sum_i D_i}{\frac{\pi}{6} \rho_f \sum_i D_i^3} \tag{9}$$

i.e.

$$\theta \;\alpha\; \frac{\sum D_i}{\sum D_i^3} \tag{10}$$

The quantity on the right side of equation 10 has dimensions of $1/(\text{length})^2$. If we use SMD of the spray as the characteristic length scale of the spray, this implies $\epsilon\,\alpha\,1/(\text{SMD})^2$. i.e. $\log\theta\;\alpha - 2\log(\text{SMD})$. This relationship is shown as a stright line in Figure 2-6.

APPENDIX C

Description of Filter Ratio Test

Fuel temperatures for Jet A and AMK are 20 ±1° C.

Apparatus: Filtration ratio apparatus as shown in Fig. C-1.

Type of filter used: 16 - 18 μ twilled Dutch weave stainless steel 164 x 1400 mesh cloth, warp diameter 0.07 mm and weft diameter 0.04 mm, pre-cut into discs of 44.5 mm diameter. The material is obtained from Tetco, Inc., 525 Montery Pass Road, Monterey Park, CA 91754.

1. Make sure filter apparatus has been rinsed clean with Jet A and then drained. Residual AMK can influence the filter time of the next sample.

2. Place an unused filter on lower filter plate, positioning it in the center so that it overlaps the edge of the orifice.

3. both 'O' rings should be properly seated. Align upper and lower filter plates the same way each time; attach lower to upper and apply screws, tightening them to the same tolerance each time.

4. Insert a rubber stopper in bottom orifice, choosing a size which does not contact the filter. Hold stopper steady until removal. Excess motion may induce gelation in the filter.

5. Tilt apparatus to diagonal and pour the reference Jet A slowly down side of tube.

6. Once tube is about 3/4 filled, return it to vertical, add fuel till it overflows into gallery.

7. Remove rubber stopper. Record time between timing reference points.

8. When apparatus has drained, replace stopper, tilt apparatus to diagonal and pour sample AMK slowly (90 seconds) down side of tube, not letting it hit bottom directly.

9. Repeat step 6.

10. Wait 60 seconds (fuel relaxation time) before removing stopper. Remove it slowly and gently with a turning motion to avoid causing suction.

11. Record time between timing reference points.

12. Dismantle lower filter plate and discard used filter. Rinse and drain apparatus.

DESCRIPTION OF FILTER SCREEN DEVICE

G-1

END

FILMED

3-84

DTIC